Towards Fabrication Information Modeling (FIM): Workflow and Methods for Multi-Scale Trans-Disciplinary informed Design

by

Jorge Duro Royo

Architect MSc., Polytechnic University of Catalonia, 2011
Mechanical Engineer MSc., Polytechnic University of Catalonia, 2010

Submitted to the Program in Media Arts and Sciences,
School of Architecture and Planning
in partial fulfillment of the requirements for the degree of

Master of Science in Media Arts and Sciences

at the

MASSACHUSETTS INSTITUTE OF TECHNOLOGY

September 2015

Signature redacted

Author .....
Program in Media Arts and Sciences,
School of Architecture and Planning
August 7, 2015

Signature redacted

Certified by .....
Neri Oxman
Associate Professor of Media Arts and Sciences
Thesis Supervisor

Signature redacted

Accepted by .....
Pattie Maes
Academic Head
Professor of Media Arts and Sciences

Towards Fabrication Information Modeling (FIM): Workflow and Methods for Multi-Scale Trans-Disciplinary informed Design

by

Jorge Duro Royo

Submitted to the Program in Media Arts and Sciences,
School of Architecture and Planning
on August 7, 2015, in partial fulfillment of the
requirements for the degree of
Master of Science in Media Arts and Sciences

Abstract

This thesis sets the stage for Fabrication Information Modeling (FIM); a design approach for enabling seamless design-to-production workflows that can derive complex designs fusing advanced digital design technologies associated with analysis, engineering and manufacturing. Present day digital fabrication platforms enable the design and construction of high-resolution and complex material distribution structures. However, virtual-to-physical workflows and their associated software environments are yet to incorporate such capabilities. As preliminary methods towards FIM I have developed four computational strategies for the design and digital construction of custom systems. These methods are presented in this thesis in the context of specific design challenges and include a biologically driven fiber construction algorithm; an anatomically driven shell-to-wearable translation protocol; an environmentally-driven swarm printing system; and a manufacturing-driven hierarchical fabrication platform. I discuss and analyze these four challenges in terms of their capabilities to integrate design across media, disciplines and scales through the concepts of multi-dimensionality, media-informed computation and trans-disciplinary data in advanced digital design workflows. With FIM I aim to contribute to the field of digital design and fabrication by enabling feedback workflows where materials are designed rather than selected; where the question of how information is passed across spatiotemporal scales is central to design generation itself; where modeling at each level of resolution and representation is based on various methods and carried out by various media or agents within a single environment; and finally, where virtual and physical considerations coexist as equals.

Keywords: Digital Design; Design Workflows; Direct Digital Manufacturing (DDM); Integrated Design; Multi-Scale Data; Trans-Disciplinary Data; Computational Design; Fabrication Information Modeling (FIM); Multi-dimensional Design Workflows; Media-informed Design Workflows; Trans-disciplinary Design Workflows

Thesis Supervisor: Neri Oxman
Title: Associate Professor of Media Arts and Sciences

Towards Fabrication Information Modeling (FIM):
A Workflow for Deriving Designs Informed by Multi-Scale Trans-Disciplinary Data
by
Jorge Duro Royo

This master thesis has been examined by a Committee as follows:

Signature redacted

Hugh Herr . .
Associate Professor of Media Arts and Sciences
Thesis Reader

Towards Fabrication Information Modeling (FIM):
A Workflow for Deriving Designs Informed by Multi-Scale Trans-Disciplinary Data
by
Jorge Duro Royo

This master thesis has been examined by a Committee as follows:

Signature redacted

Hiroshi Ishii .....
Jerome B. Wiesner Professor of Media Arts and Sciences
Thesis Reader

Acknowledgments

I dedicate this thesis to my family. To my late mother for her unconditional love, to my father for his challenging support, to my three siblings for their sense of humor and for everything they have taught me, and specially to my wife for taking me where I am today.

I would like to thank my advisor Prof. Neri Oxman for her infinite support of my work, and my readers Prof. Hugh Herr and Prof. Hiroshi Ishii for their thesis advice. I also thank my graduate and undergraduate colleagues at the Mediated Matter Group, specifically Markus Kayser, Jared Laucks, Daniel Lizardo, Sunanda Sharma, Carlos Gonzalez de Uribe, Steven Keating, William Patrick, John Klein and Chikara Inamura, as well as fellow research assistants Katia Zolotovski and Swati Varshney at the MIT Ortiz Lab. I truly appreciate collaborators Prof. Christine Ortiz (MIT DEMS), Prof. Mary C. Boyce (Columbia Engineering), Dr. James Weaver (Harvard Wyss Institute), Dr. Javier G. Fernandez (Harvard Wyss Institute), and Dr. Fiorenzo Omedetto (Tufts University). The MIT Center for Bits and Atoms provided some of the fabrication technologies for the realization of some of the projects presented here. Partial support for this thesis comes from the NSF EAGER Grant Award No.115G550 Bio-Beams: Functionally Graded Rapid Design / Fabrication, the US Army through the MIT Institute for Soldier Nanotechnologies (Contract No. W911NF- 13-D-0001), the Institute for Collaborative Biotechnologies (Grant No. W911NF-09-0001 from the US Army Research Office), the National Security Science and Engineering Faculty Fellowship Program (Grant No. N00244-09-1-0064), and the TBA-21 Academy (Thyssen-Bornemisza Art Contemporary).

Contents

1 Introduction **13**

1.1 Issues in Design of Physical Feedback Workflows 13

1.2 Intended Contributions 14

1.2.1 Integrated Design across Media, Scales and Disciplines 14

2 Background **17**

2.1 Towards Multi-dimensional, Media-informed, and Trans-disciplinary Design Workflows 17

2.1.1 Multi-scalar Design Workflows 17

2.1.2 Fabrication-informed Design Workflows 17

2.1.3 Material-informed Design Workflows 18

2.1.4 Trans-disciplinary Design Workflows 18

3 Design Workflows across Media, Disciplines, and Scales **19**

3.1 Exemplar Cases of FIM 19

3.2 Biologically driven Fiber Construction Algorithm (FCA) 20

3.2.1 FCA Digital Implementation Details 20

3.2.2 FCA Mechanics and Materials Details 21

3.2.3 FCA Biologically driven Fiber Construction Algorithm 22

3.2.4 FCA Discussion 24

3.2.5 FCA Model Results 25

3.3 Anatomically driven Shell-to-Wearable Translation Protocol (STP) 25

3.3.1 STP Biological Analysis Details 25

3.3.2 STP Digital Translation Details 26

3.3.3 STP Anatomically driven Shell-to-Wearable Translation Protocol 26

3.3.4 STP Discussion 33

3.3.5 STP Model Results 34

3.4 Environmentally driven Swarm Printing System (SPS) 36

3.4.1 SPS Digital Implementation Details 36

3.4.2 SPS Mechanics and Materials Details 37

3.4.3 SPS Environmentally driven Swarm Printing System 37

3.4.4 SPS Discussion 42
3.4.5 SPS Model Results 42
3.5 Manufacturing-driven Hierarchical Fabrication Platform (HFP) 44
3.5.1 HFP Digital Implementation Details 44
3.5.2 HFP Mechanics and Materials Details 45
3.5.3 HFP Manufacturing-driven Hierarchical Fabrication Platform 46
3.5.4 HFP Discussion 53
3.5.5 HFP Model Results 55

4 Towards a FIM Methodology **59**
4.1 Analysis of Exemplar Cases of FIM 59
4.2 Multi-dimensional Characteristics 59
4.3 Trans-disciplinary Data Integration 60
4.4 Media-informed Computation 62

5 Reflections on Fabrication Information Modeling (FIM) **63**
5.1 Future Work Towards FIM 63
5.1.1 FCA Model Future Work 64
5.1.2 STP Model Future Work 64
5.1.3 SPS Model Future Work 64
5.1.4 HFP Model Future Work 64

Chapter 1

Introduction

1.1 Issues in Design of Physical Feedback Workflows

Recent advances in digital fabrication present an exciting opportunity to merge digital and physical tools and processes in the service of achieving high degrees of design customization across scales. However, the limitations associated with computational design tools for modeling geometrically complex and materially heterogeneous structures across scales frame and limit further progress (Oxman [2011], Duro-Royo et al. [2014b], Oxman et al. [2015]). Specifically, the gap between virtual and physical platforms restricts integrated feedback across media, and limits invention and imagination of new designs and production processes (Duro-Royo et al. [2014a]).

Researchers in the fields of architectural design and advanced manufacturing are working towards the integration of material and fabrication constraints in the design process (Oosterhuis [2004], Chiu and Yu [2008]). Academic institutions and industry are rapidly developing complex multi-material manufacturing hardware able to incorporate material constraints, presenting software designers technical challenges in taking full advantage of novel hardware capabilities (Shapiro et al. [2004, 2011], Chiu and Yu [2008]). Such challenges are due to the fact that conventional computer-aided design (CAD) tools can enable and support the manipulation of geometric and topologic virtual constructs; however, they generally lack the means to embed material data within virtual model constructs (Biswas et al. [2004], Duro-Royo et al. [2015a]) mostly since material homogeneity is typically assumed (Chiu and Yu [2008]).

CAD tools, techniques and technologies are typically representation-oriented. As a result, digital design practices are generally governed by form generation prioritizing geometrical constraints over materially informed and fabrication-driven parameters (Sola-Morales [2000], Mitchell [2001]). Combined with a shape-centric process, each CAD kernel - the software's core functionalities - is typically based on a strict set of low-level mathematical and geometrical definitions. These definitions provide a certain "style" to the software package that can be easily identified and traced in its design outcomes (Mitchell [2001], Burry et al. [2002], Mogas-Soldevila [2013]).

For instance, due to embedded mathematical descriptions of software solutions, mesh-based CAD users are more likely to generate free-form designs with high degrees of agility (e.g. in Maya-Autodesk). NURBS-based CAD users, however, are more likely to generate smooth curve and surface designs like the ones that typically describe the surfaces of automobiles or water vessels (e.g. Rhino-McNeel, SolidWorks-Dessault). I claim that such stylistic underpinnings may actually limit the user's ability to conceive new design approaches. More importantly, CAD models, even if inhabiting a dimensionless virtual space, are scale-dependent due to representation tolerances embedded in their base package (Beckett and Babu [2014]). It is true though that mainstream CAD software packages, such as Autocad-Autodesk or Rhino-McNeel, allow virtual direct export and manipulation of engineering analysis (CAE) and machine instruction generation (CAM) information via scripting or parametric design plug-ins such as Dynamo or Grasshopper, respectively.

However, despite the overall successful integration of parametric design workflows in practice, as can be seen in facade construction, environmental benchmarking or structural optimization; parametric design for truly "buildable" projects remains labor-intensive, slow, and rather manual. Furthermore, such digital workflows become particularly challenging to author and to manage when dealing with more than fifty to a hundred variables (Andia and Spiegelhalter [2015]). Consequently, it becomes extremely challenging to navigate, control, adjust and compare between parameters within a single model - and even within the same software package. This is due to the design process engaging multiple dimensions including those that are directly informed by fabrication and material parameters and those that span across scales or functional domains. If new capabilities for embedding multiple dimensions of and across media, disciplines and scales were in place, designers would be able to tailor material properties to environmental constraints in close association with the digital fabrication platform. Consider, for example, the ability to tune microfiber arrangements within architectural wood columns; or the ability to concurrently shape products at scales relevant to human ergonomics, body shape and tissue composition, spanning functional and fabrication scales - environment to body to voxel.

1.2 Intended Contributions

1.2.1 Integrated Design across Media, Scales and Disciplines

I have coined the term Fabrication Information Modeling (FIM) to define the materialization of geometrically complex designs that span various media, scales, and disciplines. Three main characteristics underline designs based on the FIM approach: (1) they incorporate variables associated with design and construction media such as physical feedback sensing, fabrication and material parameters; (2) they operate across multiple dimensions; and, (3) they integrate and manage transdisciplinary data parameters, constraints, or data sets from multiple disciplines. With FIM, I aim to design and build physical feedback workflows where materials are designed rather than selected;

where the question of how information is passed across spatiotemporal scales is central to the design generation process itself; where modeling at each level of resolution and representation is based on various (and often complimenting) methods, and performed by different agents within a single environment; and finally, where virtual and physical considerations coexist as equals.

Chapter 2

Background

2.1 Towards Multi-dimensional, Media-informed, and Trans-disciplinary Design Workflows

2.1.1 Multi-scalar Design Workflows

Multi-scalar design is an emerging field of research in the disciplines of Materials Science and Engineering, Civil Engineering, and Synthetic Biology. Consider, for example, research into the mechanics of deformation and failure of biological materials. Such research integrates computational modeling of material properties from atomic scale to meter scale by examining fundamental links between processes, structures, properties and functions (Cranford and Buehler [2012]). Other efforts aim to bridge the gap between modeling and simulation of products involving multiple physical processes interacting at multiple spatial and temporal scales such as research associated with the design and construction of fan blades, turbo-engines, or car chassis (Fish [2013]). Furthermore, novel initiatives in computational biotechnology seek to examine living systems, considering dimensions of multi-scale data, to advance our understanding of how human bodies function (Kidd et al. [2014]).

2.1.2 Fabrication-informed Design Workflows

In the pursuit of incorporating fabrication constraints into the design process, File-to-Factory approaches aim to merge CAD (Computer-aided Design) and Computer-aided Manufacturing (CAM) into a seamless process (Oosterhuis [2004], Oosterhuis et al. [2004], Afify et al. [2007], Scheurer [2010]). This is commonly achieved by exporting the virtual design into a specific machine file format (Chang [2004], Sass and Oxman [2006], Sheil [2013]). Following, materials and tool paths are set within the machine's software with limited possibility for iterations; as well as incompatibilities between the original CAD environment and the machine logic that are lost in translation. Such discrete processes are all but seamless, constraining and directing the workflow of designs that are complex in shape and in material composition (Oxman [2011], Duro-Royo et al. [2015a]).

2.1.3 Material-informed Design Workflows

Current efforts in the area of structural design that focus on achieving material-informed architectural design processes, aim at better understanding and expressing the performance of existing material systems and incorporating it into shape-generating parametric models (Fleischmann et al. [2011], Schleicher et al. [2015]). This is typically done by experimentally studying functional-morphological dependencies of systems such as plywood or fiber-based composites in abstract load simulation setups. Following, approximated models are built and evaluated via virtual structural analysis tools (Schleicher et al. [2015]). Such digital chains depend on simulation methods that are difficult to implement with precision, and that generally respond to a narrow set of framing conditions. Moreover, the relevance of these workflows to the quality of the product lies at the structural scale, rather than the scale of material property. In the area of additive manufacturing, researchers combining software logic and digital fabrication claim that soon it will be possible to use multi-material printers and nanotechnology to design completely new materials whose behavior can be programmed (Andia and Spiegelhalter [2015]). Despite all these efforts, fully integrated, material-driven digital models are yet to be implemented in off-the-shelf software to enable design processes that are fully informed by material behavior (Schleicher et al. [2015], Tamke et al. [2013]).

2.1.4 Trans-disciplinary Design Workflows

The success of research developments reviewed above is highly dependent on efficient and timely incorporation of trans-disciplinary information. Design thinking is generally considered a non-linear process with multiple parameters; a process that incorporates diverse disciplinary knowledge such as, for instance: structural analysis via engineering of behavioral models (Kara and Georgoulias [2012]); complex performance evaluation via biologically inspired algorithms (Turrin et al. [2011]); geometric function negotiation via morphometric analysis techniques (Duro-Royo et al. [2014b]); structural property tailoring via materials engineering across scales (Cranford and Buehler [2012], Fish [2013]); digital fabrication via form interpretation into machine code (Chang [2004]); or even understanding innovation via techniques from social sciences (Nelson et al. [2006]). Workflows that seamlessly embed and operate with data from other disciplines are far more suitable to adapt and respond to contemporary issues, and to convert complex architectural design process into multi-agent discussions rather than tedious information translations.

Chapter 3

Design Workflows across Media, Disciplines, and Scales

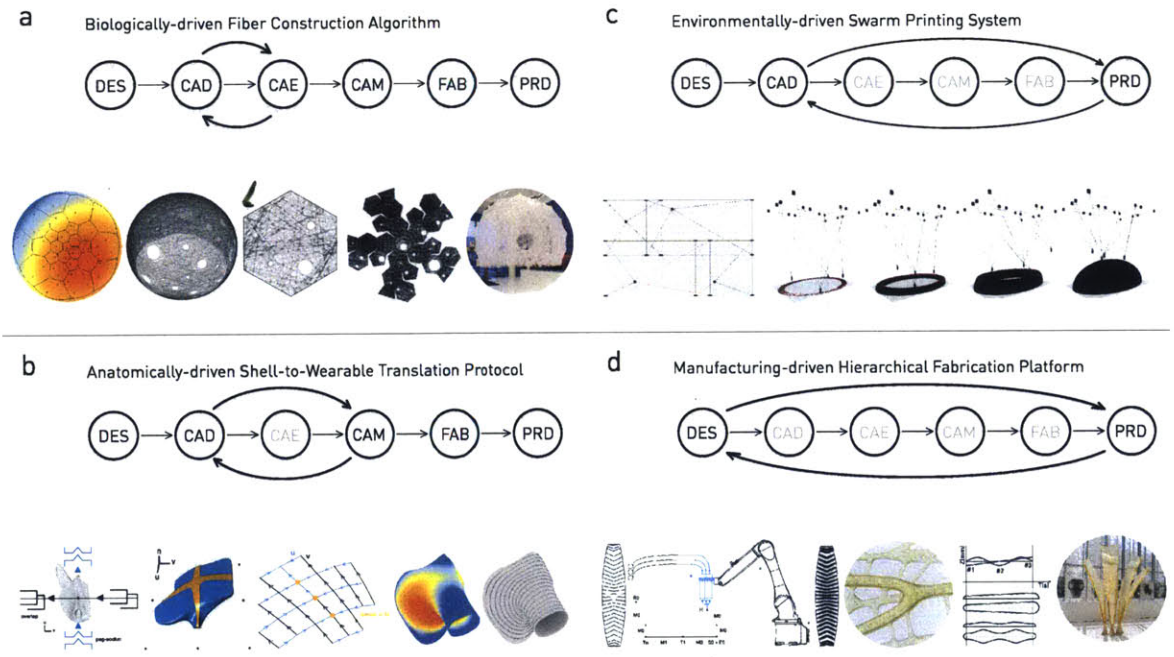

Figure 3-1: Four exemplar cases as steps towards a FIM methodology; (a) a biologically driven fiber construction algorithm (FCA); (b) an anatomically driven shell-to-wearable translation protocol (STP); (c) an environmentally driven swarm printing system (SPS); and (d) a manufacturing-driven hierarchical fabrication platform (HFP). Figure from Duro-Royo et al. [2015b].

3.1 Exemplar Cases of FIM

I demonstrate the principles for the FIM methodology in four customized experimental workflows: (1) a biologically driven fiber construction algorithm; (2) an anatomically driven shell-to-wearable translation protocol; (3) an environmentally driven swarm printing system; and, (4) a

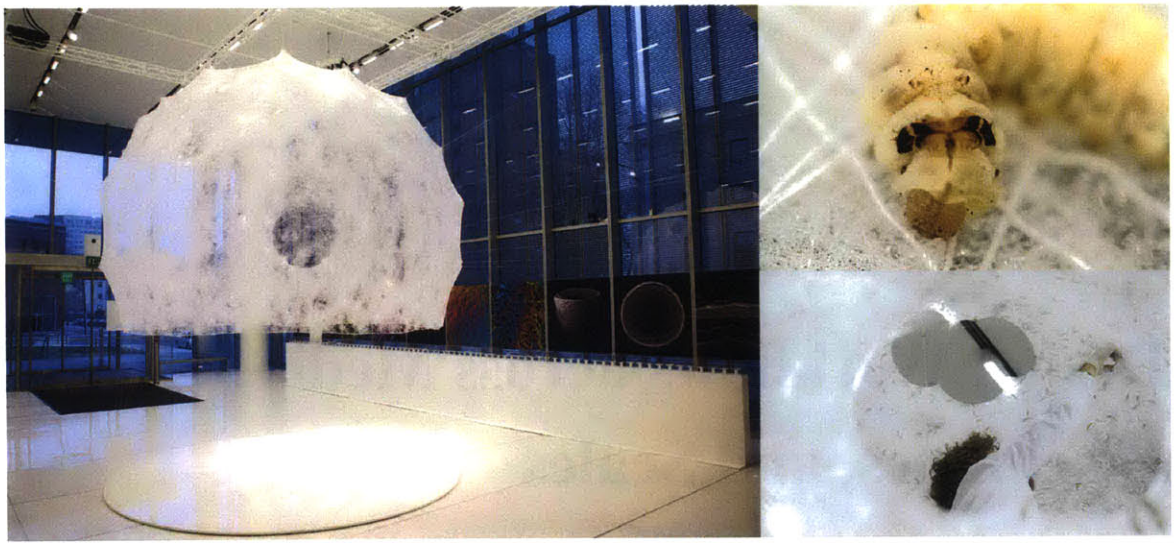

Figure 3-2: The Silk Pavilion, Mediated Matter Group, MIT Media Lab 2013.

manufacturing-driven hierarchical fabrication platform (Figure 3-1). The methods are implemented combining custom applets in C, C++, C# and Java languages using the Eclipse IDE and VisualStudio environments (The Eclipse Foundation 2004), as well as C# scripts using the RhinoCommon geometrical kernel (McNeel 2010). The resulting designs are fabricated with advanced additive manufacturing hardware using commercial and customized tools, techniques and technologies.

3.2 Biologically driven Fiber Construction Algorithm (FCA)

The goal of the FCA model is to design and fabricate a fiber-based large-scale structure (Figure 3-2, (Figure 3-1a)) that explores the relationship between digital and biological fiber-based fabrication integrating three sets of constraints, namely: environmental parameters relating to solar radiation; physiological parameters relating to the silkworm spinning process; and manufacturing parameters relating to a computer-controlled fabrication machine (Figure 3-3). The model is designed to integrate biological spinning and robotic construction into a composite structure made of both natural and industrial silk (more information on the computational model can be found in Oxman et al. [2013a]).

3.2.1 FCA Digital Implementation Details

The generative environment includes a new library designed on top of the RhinoCommon build that runs on the Grasshopper plug-in (in McNeel Rhinoceros 3D-Modeler). The library comprises a set of routines that enable the shaping of lightweight fibrous environments. Three data sets informed the algorithm. The first set contains where fabrication-driven informed by a CNC manufacturing platform along with its prescribed gantry size and tool reach. This set generated the need for a spherical structure of the pavilion to be subdivided into a set of sub-structural patches. The patches

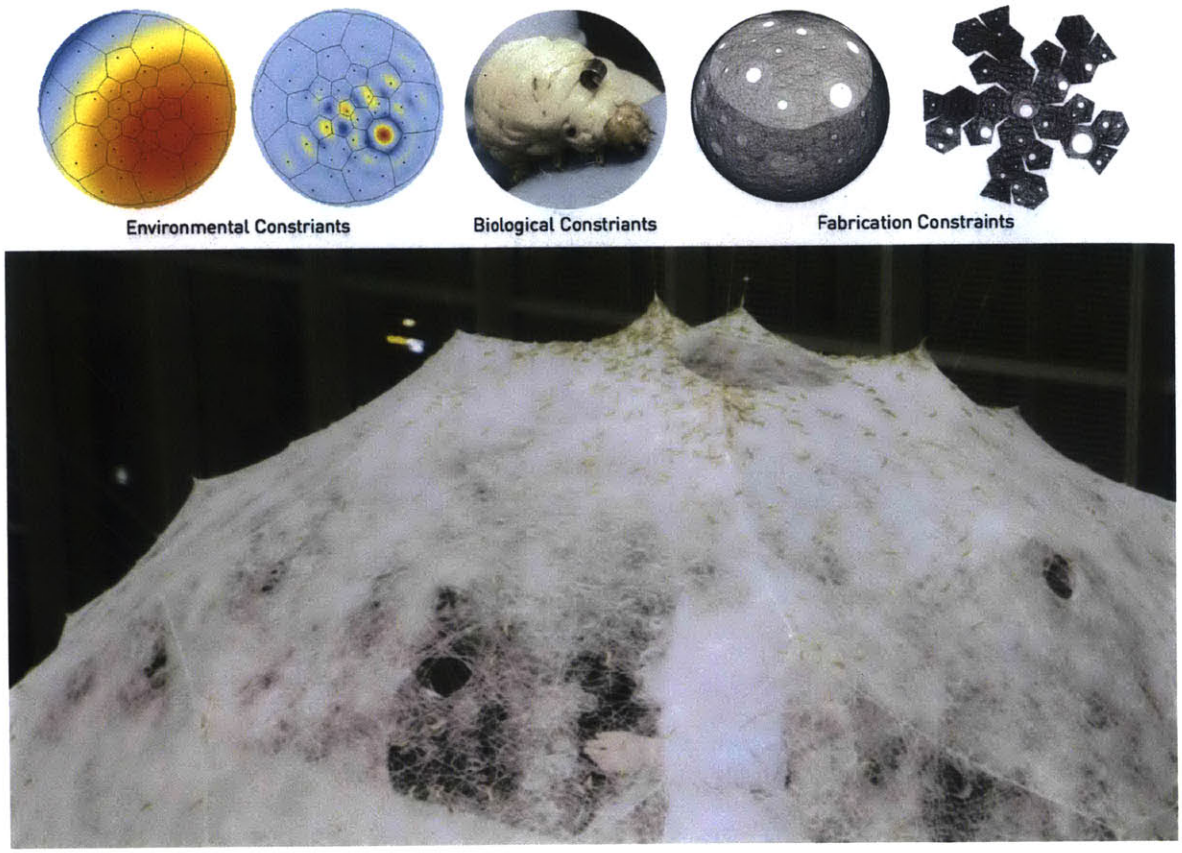

Figure 3-3: The FCA model integrates three sets of constraints: environmental parameters relating to solar radiation; physiological parameters relating to the silkworm spinning process; and manufacturing parameters relating to computer-controlled fabrication.

conformed to a truncated icosahedron whose faces fit the robotic manufacturing bed. The second set of constraints originated in two data maps; the first map encoded the specific on-site solar trajectory and the second provided an opening radius multiplier to generate organizational fiber variation. Combined, these two maps informed the position and size of the pavilion apertures (Figure 3-4). The third set of constraints is linked to the silkworm's biological characteristics; with the goal of providing maximum silk deposit reach (Oxman et al. [2013a]).

3.2.2 FCA Mechanics and Materials Details

Mechanics: The primary structure resulting from the FCA model is comprised of 26 polygonal panels (Figure 3-6f) mechanically woven by a CNC (Computerized Numerical Control) machine. The overall geometry is created using an algorithm that assigns a single continuous thread (Figure 3-6e) across the panels (Figure 3-6c), Figure 3-6d), providing fiber density gradients informed by environmental constraints of light and heat (Figure 3-6a, Figure 3-6b).

Materials: The base scaffolding is generated with industrial woven silk and final density variation is obtained by deploying 6500 Bombyx mori silkworms as a biological material factory in the

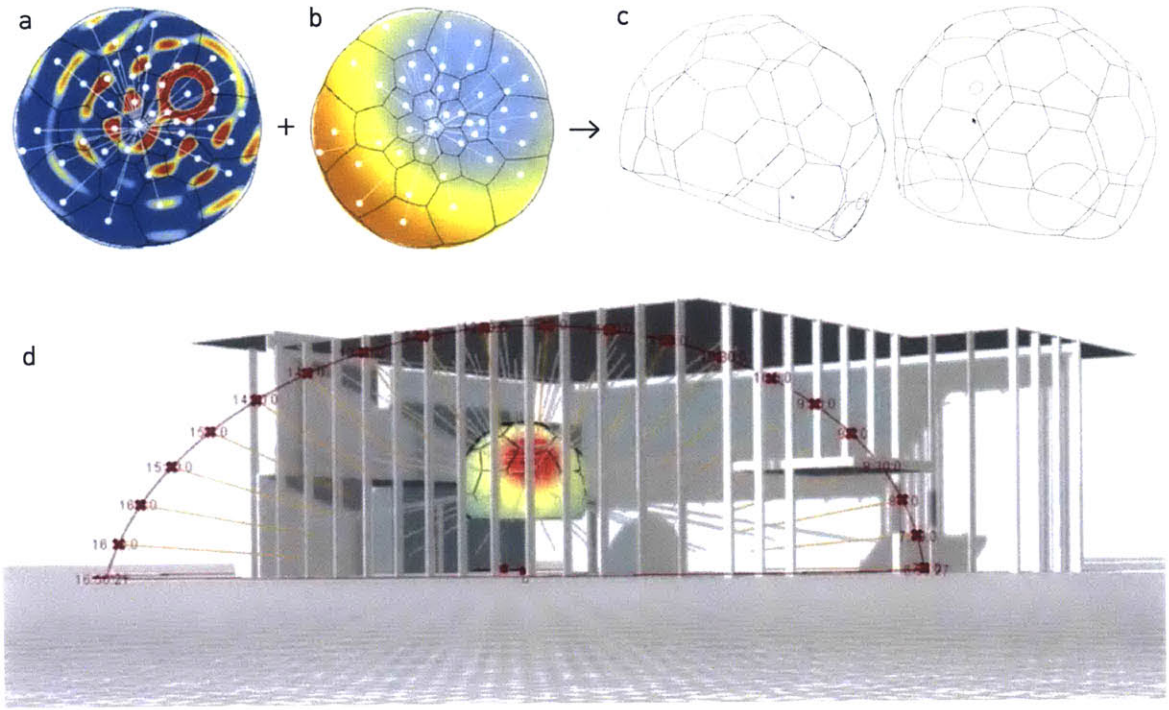

Figure 3-4: Captures of the FCA model design applet: (a) Solar mapping analysis. (b) Aperture mapping analysis. (c) Resulting design configuration. (d) Design and environmental analysis visualized on project site.

creation of a reinforcing secondary fiber structure on top of the CNC-woven scaffold (Figure 3-2) (Oxman et al. [2013a]).

3.2.3 FCA Biologically driven Fiber Construction Algorithm

The pavilion is designed and constructed in two phases: the first phase consists of digitally fabricating a scaffolding envelope made of industrially-produced silk fibers and the second phase consists of deploying thousands of silkworms to spin a secondary naturally-produced silk envelope. A set of apertures built into the initial envelope capture environmental light and heat controlling the distribution of silkworms on the structure. Figure 3-4 shows the FCA design applet where apertures are defined according to environmental solar path analysis. Overcoming current limitations of existing computer aided design (CAD) tools; a parametric environment is developed that facilitates the design and fabrication phases of the project, enabling continuous iteration between digital form-finding and physical fabrication processes. The FCA's set of algorithms also serve to mediate between environmental input (Figure 3-4a, Figure 3-4b), material properties and organization (Figure 3-5), biological fabrication constraints ((Figure 3-3), as well as real-time evaluation of multiple design solutions (Oxman et al. [2013a]).

The main goal of FCA is to develop a holistic computational design environment able to simultaneously process multiple sets of complex constraints in real time. Most of these constraints are difficult or impossible to capture using current CAD tools. For instance, the ability to automatically

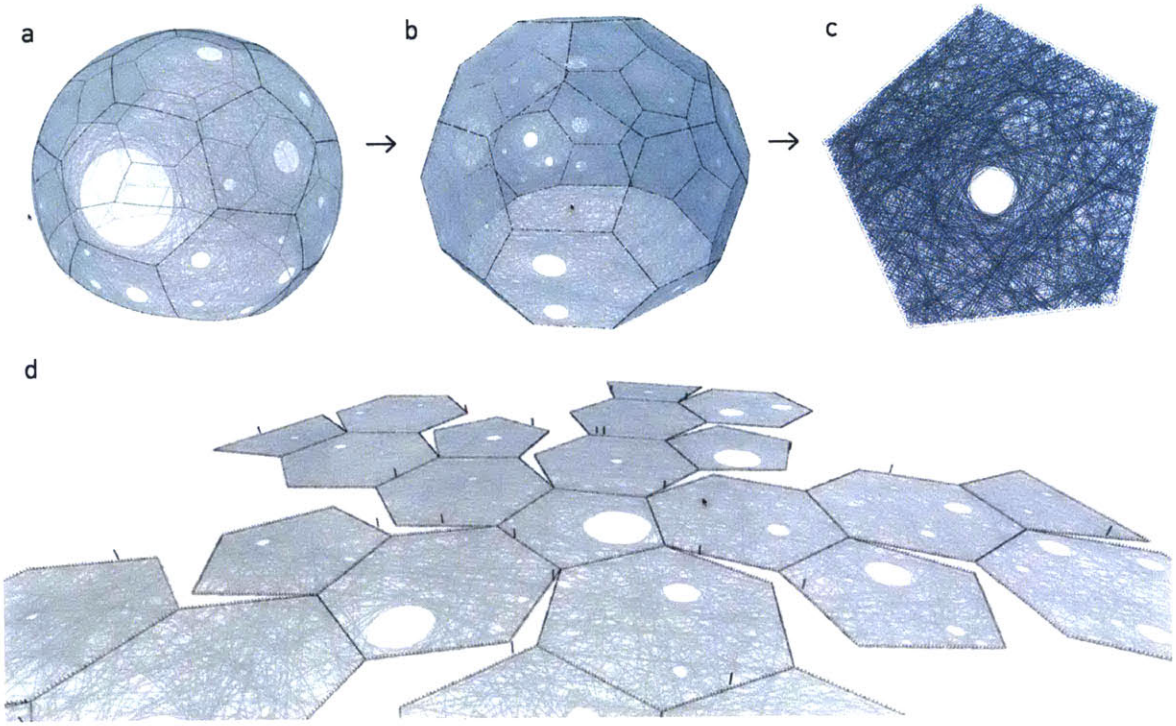

Figure 3-5: Captures of the FCA model design applet: (a) Fiber-based scaffolding design result. (b) Polygonalization of the design result for fabrication. (c) CNC weaving tool-paths for a single polygon. (d) CNC weaving tool-paths for all 26 polygonal panels.

determine, for every digitally woven fiber, what space the silkworm can spin, enabling convergence between the digitally laid silk fibers and the biologically spun ones. Another goal is to computationally embody the geometrical complexity and scalability of the Pavilion, as well as the scaffolding resolution within the gantry of fabrication tools used. The resulting design environment applet informs the designer about overall material organization as well as the effects of the biological parameters (such as silkworm motion range) on the final design (Figure 3-4, Figure 3-5) (Oxman et al. [2013a]).

For each aperture positioned according to the site's light conditions, the FCA protocol identifies a continuous tangent circle on the spherical geometry (Figure 3-6c). It is then converted into tangent line segments, represented in 2D, matching the patch fabrication. For each circle, a parameter controlling the resolution of the tangents is assigned that determines the ratio between local fiber gradients to overall fiber distribution and organization (Figure 3-5a). The algorithm then checks each aperture to find out if it is contained within a prescribed patch, multiple patches or none, and classifies this information as data lists (Figure 3-5b). For each patch containing a full or partial aperture, the algorithm computes the following: (I) Aperture formation in relation to the overall image of a continuous thread (Figure 3-6e). (II) Thread redistribution across apertures, providing balance between aperture distribution and continued thread allocation across the surface area of the overall volume. (III) Contour attachments for local continuous threads (Figure 3-5c). (IV) Scaffolding thread-spacing conformation to biological parameters of the silkworm weaving pattern (Figure 3-

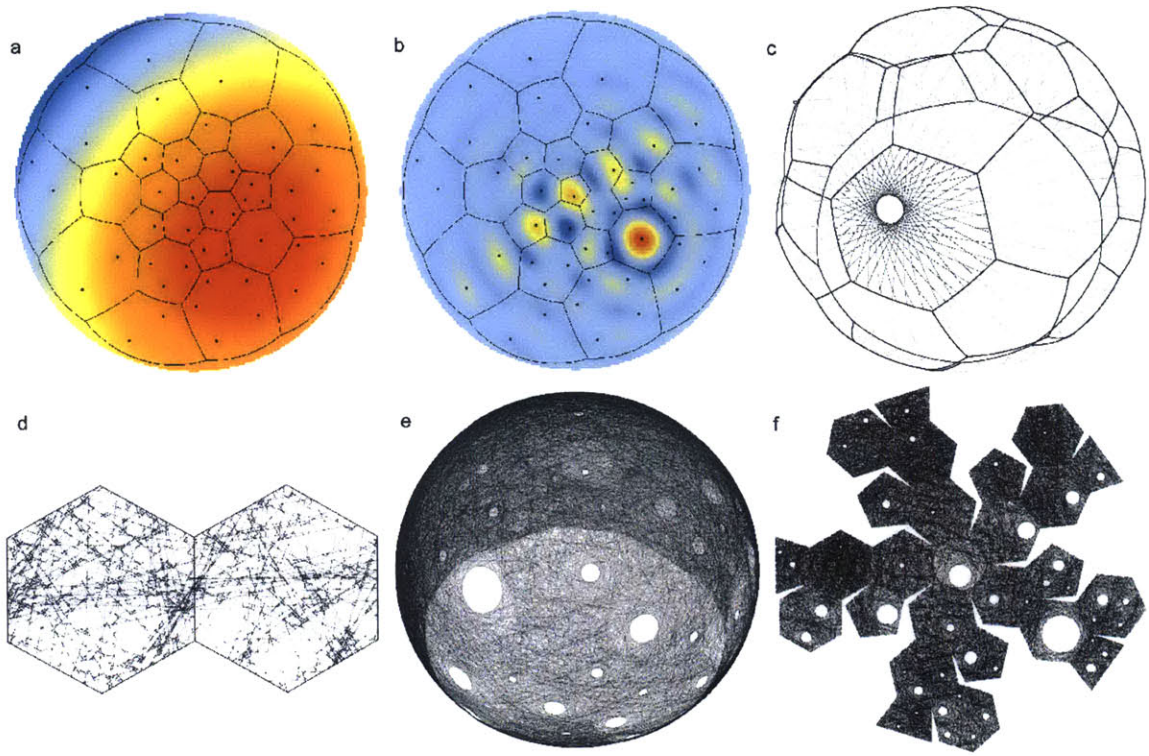

Figure 3-6: FCA model steps. (a) Computational projection of paneled dome: solar mapping. (b) Computational projection of paneled dome: aperture distribution mapping. (c) Computational generation logic of single aperture. (d) Computational silkworm spinning range calculation. (e) Final computational path with global aperture distribution. (f) Computational unfolded overall panel layout for fabrication.

6d). (V) Robotic tool-path for fabrication (Figure 3-5d). A final overall visualization of the pavilion, aluminum frame profiles for water jet manufacturing of the unfolded panels, and unfolded tool-paths for CNC weaving are then generated as output (Figure 3-6f) (Oxman et al. [2013a]).

3.2.4 FCA Discussion

The Silk Pavilion explores the duality of digitally and biologically fabricated structures by proposing a template construction approach to fiber-based digital fabrication. In this approach, the FCA digital tools are implemented to deliver a highly differentiated scaffold, on top of which a biological system is deployed. The two systems are complimentary: while one provides the load-bearing paths of the structure, the other strengthens these trajectories and acts as a skin. Moreover, the biologically deposited silk embodies qualities associated with its scale that could not have been achieved using current digital fabrication tools. The silkworm-spun non-woven fibroin adheres to and wraps around the digitally deposited silk fibers and provides for a fibrous infill due to the interaction between the two chemical agents deposited by the silkworm: the fibroin that acts as fiber and the sericin that acts as glue or connective tissue. For further information on biological experimentation conducted by the MIT Mediated Matter Group refer to (Oxman et al. [2013a]).

3.2.5 FCA Model Results

The templated construction approach presented can be implemented using other types of digital fabrication tools and biological systems. In this respect, the FCA computational model that I developed for this project is considered a generative one: it can address other similar problems across a range of scales and across an array of fabrication methods, environments and biological systems of choice, importantly pointing towards a new design workflow characteristic of Fabrication Information Modeling (FIM). Several potential applications may be considered as possible outcomes of this research (Oxman et al. [2013a]).
With regard to the direct potential for biological fabrication combined with digital fabrication, there is an interesting relationship between scaffold morphology and deposited biological fiber organization that can be considered most valuable (Figure 3-2). This, not only bypasses the processing of silk cocoons into thread and textile, but also promotes a more sustainable silk harvesting cycle (Oxman et al. [2013a]).

3.3 Anatomically driven Shell-to-Wearable Translation Protocol (STP)

The goal of the STP model in collaboration with the MIT Ortiz Group is to design an armored system composed of overlapping and interlocking units that can adapt to any surface. Data is obtained by analyzing the scales of a prehistoric fish exoskeleton. In the fish scale system differentiated geometric features and varying material properties achieve a dual function of flexibility and protection. Observed levels of sophistication are quantified and incorporated into a mesh data structure adapted to the human chest that can generate a new scale system from geometric metadata embedded in its vertices (Figure 3-1b) (more information on the computational model can be found in Duro-Royo et al. [2014b]) (Duro-Royo et al. [2015b]).

3.3.1 STP Biological Analysis Details

X-ray Micro-computed Tomography (uCT) : Eleven scales are excised from a deceased P. senegalus specimen (every 10th scale across a row on the left side of the body) and scanned via x-ray micro-computed tomography (uCT; Viva CT40, Scanco Medical AG, Switzerland) operated at 45kV and 177uA. The microtomographic data is reconstructed using bilinear and interplane interpolation algorithms into polygonal meshes using interactive medical imaging software (MIMICS 14.1, Materialise, Belgium) to generate digital 3D objects of the scales in sterolithography (STL) format. Further processing is executed in Rhino3D (Rhino-McNeel and Associates, USA) to remove noise and internal porosity. For more information on scientific analysis conducted by MIT Ortiz Group students please refer to (Duro-Royo et al. [2014b]).
Morphometric Analysis : Geometric analysis measured variation in scale shape and served as a basis for the computational model. The coordinates of twenty landmarks defining the outline of the scale including all geometrical features are extracted from the 3D STL objects using a custom

Visual Basic code programmed in the Rhino3D environment. These landmark coordinates are subjected to translation, rotation, and scaling relative to the centroid. Magnitudes of relative geometric parameters are calculated based on the coordinates. The volume of the scale is measured from the STL file in Rhino3D (Duro-Royo et al. [2014b]).

3.3.2 STP Digital Translation Details

Computational Modeling : The computational framework defining the STP data structure (local scale geometric definition, regional directionality patterns, and global functional gradient application) is implemented in C# on top of the design platform in Rhino3D. The mesh optimization process is implemented in Java (Eclipse IDE, 2013 The Eclipse Foundation) and deployed within a customized applet (Duro-Royo et al. [2014b]).
Multi-material 3D Printing : The closed-surface multi-material prototypes are designed using parametric CAD software (SOLIDWORKS, Dassault Systmes SolidWorks Corp., France) as described by Reichert et al. for a flat surface (Reichert [2010]). The components of the prototype are exported as separate STL files per material component and fabricated using multi-material 3D printing (using digital materials from OBJET Connex500TM) with 30um resolution in the digital mode. Rigid components are printed with VeroWhite (Objet FullCure 830) and compliant components are printed with TangoPlus (Objet FullCure 930) (Duro-Royo et al. [2014b]).

3.3.3 STP Anatomically driven Shell-to-Wearable Translation Protocol

Our hierarchical computational model, STP, unpacks the organism-specific design principles and applies them, in a generative way, to a different host surface with new functional specifications. STP creates and maintains consistent neighborhood relationships for the three-dimensional articulated surfaces of units on a quadrilateral polygonal mesh. The mesh data structure tailored for this model is designed to meet specific topological, algorithmic, and data access requirements.
The topology of the structure is a high-resolution polygonal regular mesh of quads with boundaries. The three components of a polygon mesh (vertices, edges, or faces) determine the connectivity between the mesh elements (Mäntylä [1988]). To ensure smooth connectivity between component features, each vertex holds one scale unit and each face shares the information of four scale geometries. I specify meshes with boundaries, defined by edges incident to only one face (Mäntylä [1983]) to include neckline and sleeve openings. The paraserial and interserial axes in the fish exoskeleton are translated onto the u- and v- directions of the parametric surface subdivision (Duro-Royo et al. [2014b]).
Algorithmic requirements operate on unit orientation and connectivity along $u-$ and $v-$ directions, as well as on unit geometry adaptation to new vertex positions through mesh optimization. Furthermore, the model takes into account functional gradients of protection and flexibility mapped on the human body. In order to preserve smooth continuity of the functional changes over the host surface, the model associates extra geometry to the vertices, edges, and faces of the mesh to share geomet-

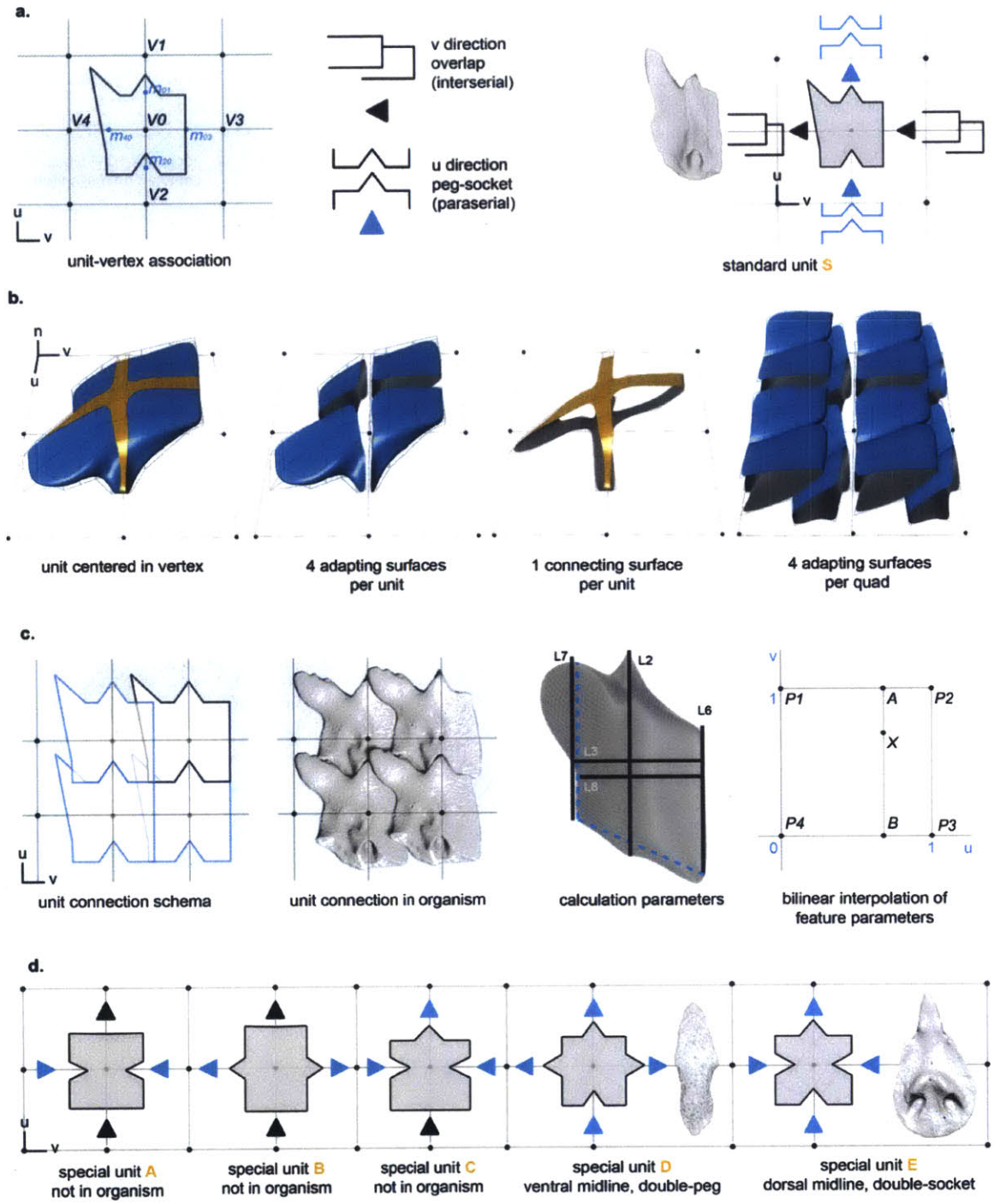

Figure 3-7: STP local unit construction. a. Vertex-centric (V0) unit placement on top of the underlying mesh and identification of u- (peg-socket) and v- (overlap) directions in the model. b. Unit construction from four connecting surfaces (blue) and a cross-shaped contact surface (orange). c. Arrangement of 4 standard units in the model and in the organism and calculation of the unit features from geometrical analysis parameters (L). d. Different specialized unit types identified by the u- and v- directions present in the organism (D, E) or defined by the directionality pattern of the new host (A, B, C). Figure from Duro-Royo et al. [2014b].

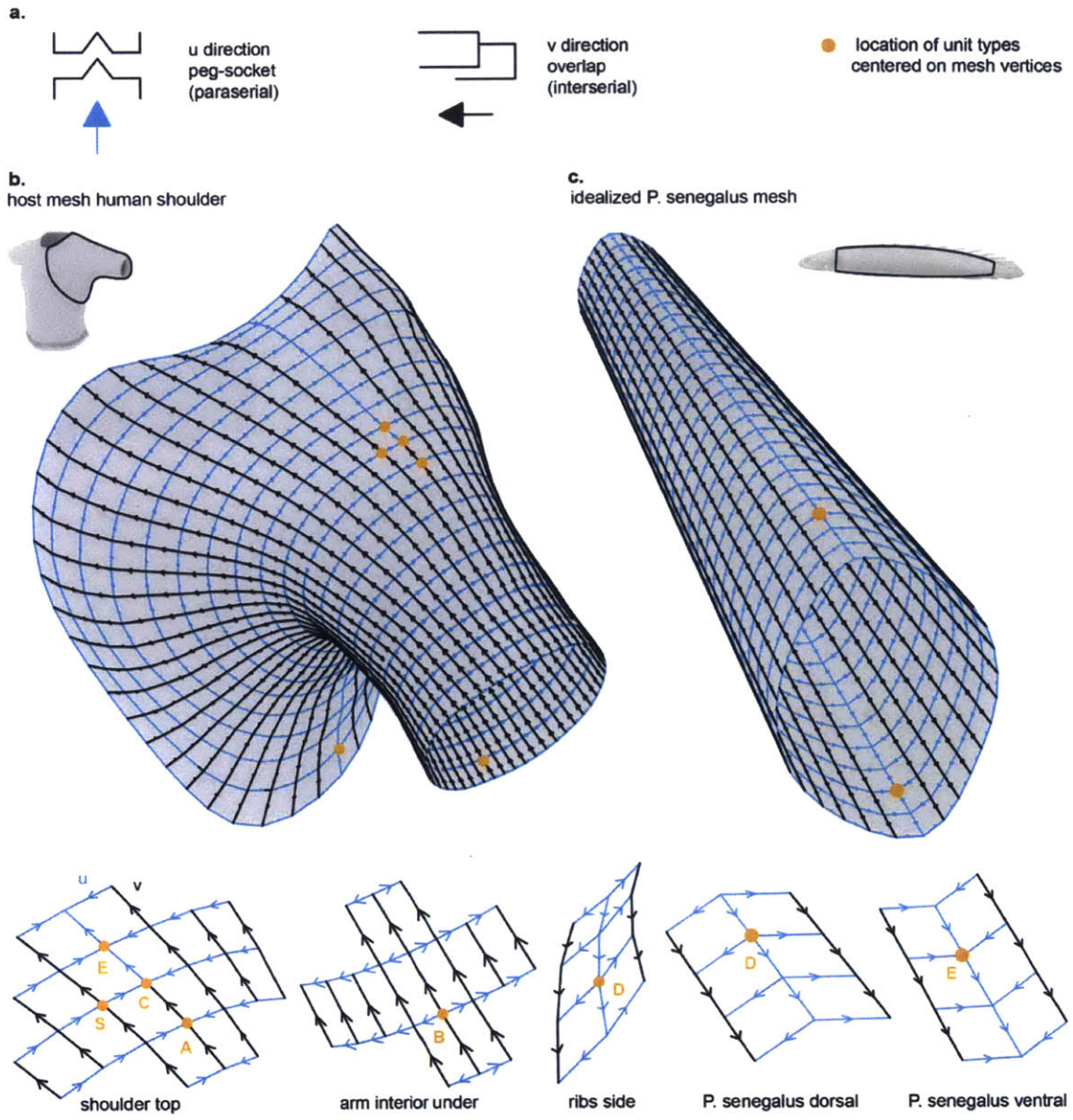

Figure 3-8: STP regional directionality pattern. a. Definition of peg-and-socket u- direction (blue arrows) and overlap v-direction (black arrows). b. Identification of directionality pattern on the human body and emergence of new specialized unit types (orange). c. u- and v- directions on the idealized tube-shaped body of P. senegalus and location of the organism's specialized units (orange). Figure from Duro-Royo et al. [2014b].

rical data with neighboring elements. To do this, I used a finite set of vertex indices (V), a table of 3D vertex coordinates $X = x_i : I \varepsilon V$, and a set of polygon faces (F), in which a face $f = (i1...inf)$ is a sequence of non-repeating vertex indices (Taubin [2012]).
I further impose access requirements to the sets of data included in the model. The data sets for vertices, edges, and faces are accessible by enumeration of all elements and the oriented transversal of face edges. Given an edge, the model is able to access its starting and end vertices. Given a vertex, at least one attached face or edge must be accessible while all other elements in the neighborhood of the vertex (i.e. incident faces, edges, or neighboring vertices) can be enumerated (Kobbelt and Botsch [2003]).
The hierarchical computational model, STP, is designed to meet these requirements at three organizational levels following the geometric rules of assembly: (i) local definition of a standard unit and construction of different unit geometries in association with their neighbors, (ii) regional application of directional patterns and functional gradients that define the locations of different units, and (iii) global optimization of the host mesh to reposition vertices that affect local adaptation of unit shapes (Duro-Royo et al. [2014b]).
Local: The local level of organization captures the standard scale unit (S) as a building block by taking into account the features of its neighbors and the underlying host mesh geometry (Figure 3-7). Each scale unit is centered on top of one mesh vertex and constructed through a set of controllable parameters (Figure 3-7a). Since each vertex has an associated unit, its geometry can adapt to the host surface curvature. The local set of information per mesh face contains shared data between four units, which takes into account the features of neighboring scales. Each vertex stores the information of four parameters that will affect its associated unit schema in two different directions. Along the u-direction (paraserial), the unit geometry is influenced by the PSL, PO, and APL parameters. Along the v- direction (interserial), the unit geometry and lateral scale superposition are influenced by IO (Duro-Royo et al. [2014b]).
Specific parametric dimensions are calculated to determine unit features and their position on the quad in order to unite the underlying mesh with the geometrical parameters and functional requirements of the host surface. A particular vertex is defined as $V_0(i,j)$, and its four neighbor vertices are defined as $V_1(u+1,v)$, $V_2(u-1,v)$, $V_3(u,v+1)$, $V_4(u,v-1)$ as shown in Figure 3-7a. The midpoints of their edges are then defined as m_{4-0}, m_{0-1}, m_{0-3}, m_{2-0}. Figure 3-7b shows how the unit is constructed from four connecting surfaces for each adjacent mesh quad (blue) and resulting cross-shaped contact surface centered in the vertex (orange). The unit lengths are calculated as shown in the table below and then mapped onto the mesh quads using a unit square bilinear interpolation algorithm (Zhang et al. [2005]), as shown in Figure 3-7c, where an unknown function f at point $X(u,v)$ is found with respect to a unit quad of points $P_1(1,0)$, $P_2(1,1)$, $P_3(1,0)$ and $P_4(0,0)$. I perform a linear interpolation between P1 and P2 resulting in point A(u,v) and another linear interpolation between point P3 and P4 resulting in point B(u,v) providing an estimate for f(u,v):

$$f(u,v) = f_{0,0} * (1-u) * (1-v) + f_{1,0} * u * (1-v) + f_{0,1} * -u * v + f_{1,1} * u * v.$$

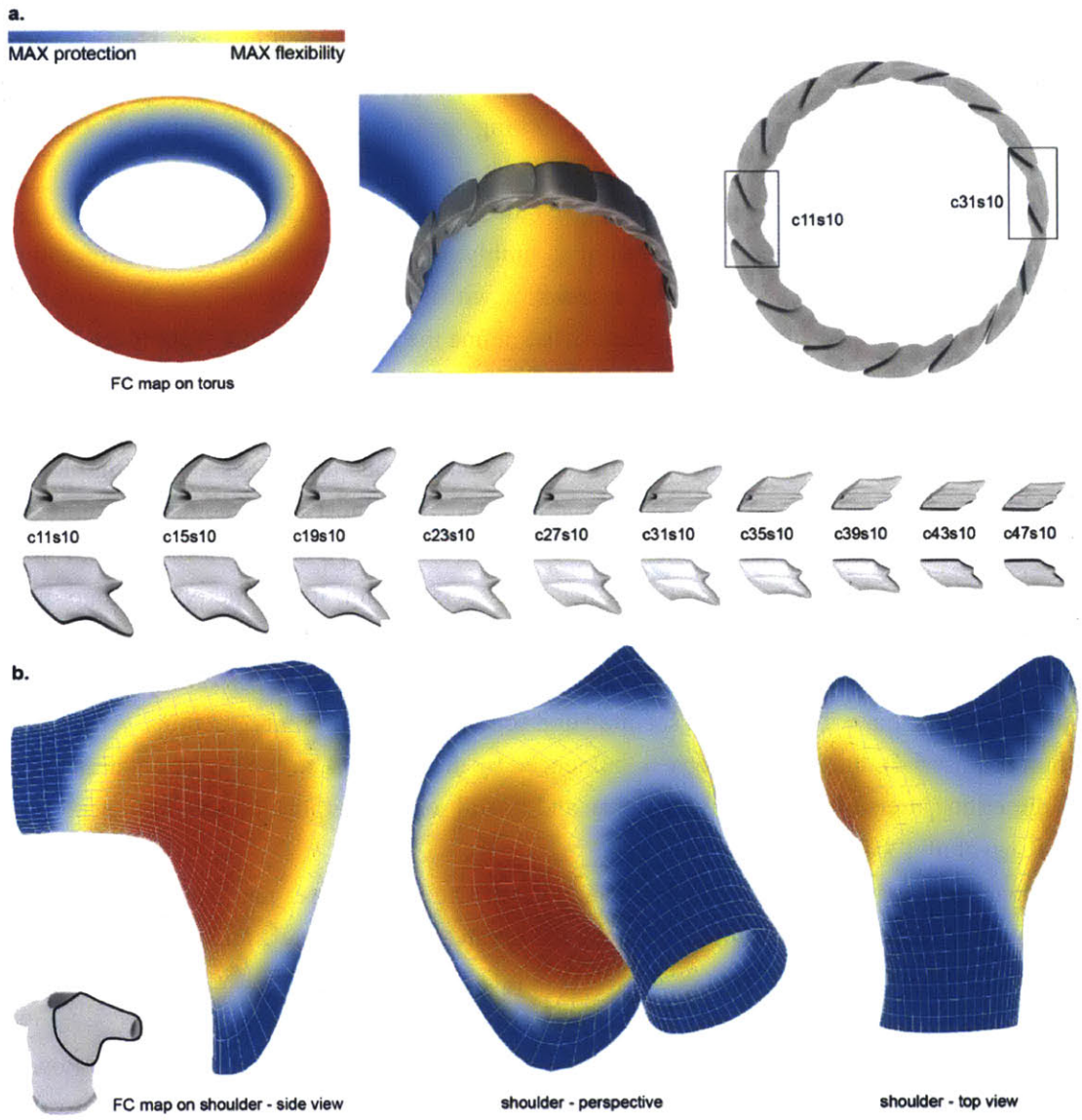

Figure 3-9: Variation of the unit features along an extreme band of Functional Coefficient (FC) mapping from maximum protection (blue) to maximum flexibility (red). a. The shape variant from head region (c11s10) and from tail region (c31s10) are mapped and morphed on the torus based on the functional gradient of FC (bottom). b. Identification of the estimated FC gradient on a human chest from maximum protection (blue) above the shoulder and maximum flexibility (red) in the underarm. Figure from Duro-Royo et al. [2014b].

Scale Width $L_8 = m_{4-0} - m_{0-3}$,

AP Length $L_6 = m_{2-0} - m_{0-1}$,

PO Length $L_7 = APL/L_6$,

Overall Length $L_2 = L_1 + L_5 + L_6$, where $L_1 = L_2 * PSL$ and $L_5 = L_2 * PO$, so $L_2 = L_6/(1-(PSL+PO))$,

Overall Width $L_3 = L_8 + L_4$, where $L_4 = L_3 * IO$, so $L_3 = L_8/(1-IO)$.

The u- and v- directions act as guides for the construction of the peg-socket and overlap connections in a unit. In STP computation each side of a quad can host either u- or v- direction and this allows definition of new types of specialized units in addition to the ones found in the fish (e.g. A, B, C in Figure 3-7d). The double-peg and double- socket units in the top and bottom midlines in the fish (e.g. D, E in Figure 3-7d) are defined as variations from the standard scale through the encoded u- and v- directions. This method of specialized units enabling polygonal mesh connectivity is similar to the stitch mesh method developed by Yuksel et al. for yarn patterns in 2.5D, where course and wale edges have an extra layer of information to define the connectivity of the yarn elements at the mesh edges (Yuksel et al. [2012]).

Regional: The regional level of organization orients mesh regions against the hosting surface. A mesh is defined as orientable if all faces (i.e. normal vectors for all polygons) point consistently to the same side of the mesh. The information encoded in the u- and v- directions does not affect the orientability of the mesh, but tailors edge directionality as extra regional data in the data structure. Figure 3-8 illustrates the directionality analysis of a human shoulder mesh in response to an estimated biomechanical logic. The u- and v- directions (Figure 3-8a) are applied to each face of the shoulder mesh (Figure 3-8b). The complexity of the host in contrast to an idealized tube mesh representing the fish body requires the emergence of more specialized units than the ones present in the P. senegalus. The locations of these specialized units that have emerged through the implementation of the STP model to the complex mesh of human body in contrast to a tube mesh representing the fish body are identified in Figure 3-8b, Figure 3-8c (Duro-Royo et al. [2014b]).

Global : The global level of organization applies optimization strategies to the hosting mesh and subsequently automates the adaptation of regional connectivity patterns and local unit shapes. To integrate functional differentiation that exists in the biological system, I assign a FC map to the mesh data structure to modulate the unit geometry of every mesh vertex toward a protective variation of heavily articulated features (blue, FC=0) or more flexible with reduced features (red, FC=1). In combination with the neighborhood relationships, this strategy allows functional gradation across the mesh. Figure 3-9a shows how the range of values of FC is translated into a sequence of scale shapes over a torus ranging from most pronounced to least pronounced relative feature size. The most protective shape variant from the head region in the fish (c11s10) and the most flexible one from the tail region (c31s10) are mapped and morphed on the torus based on the functional gradient of FC. Figure 3-9b illustrates the mapping of the FC gradient into the human shoulder mesh

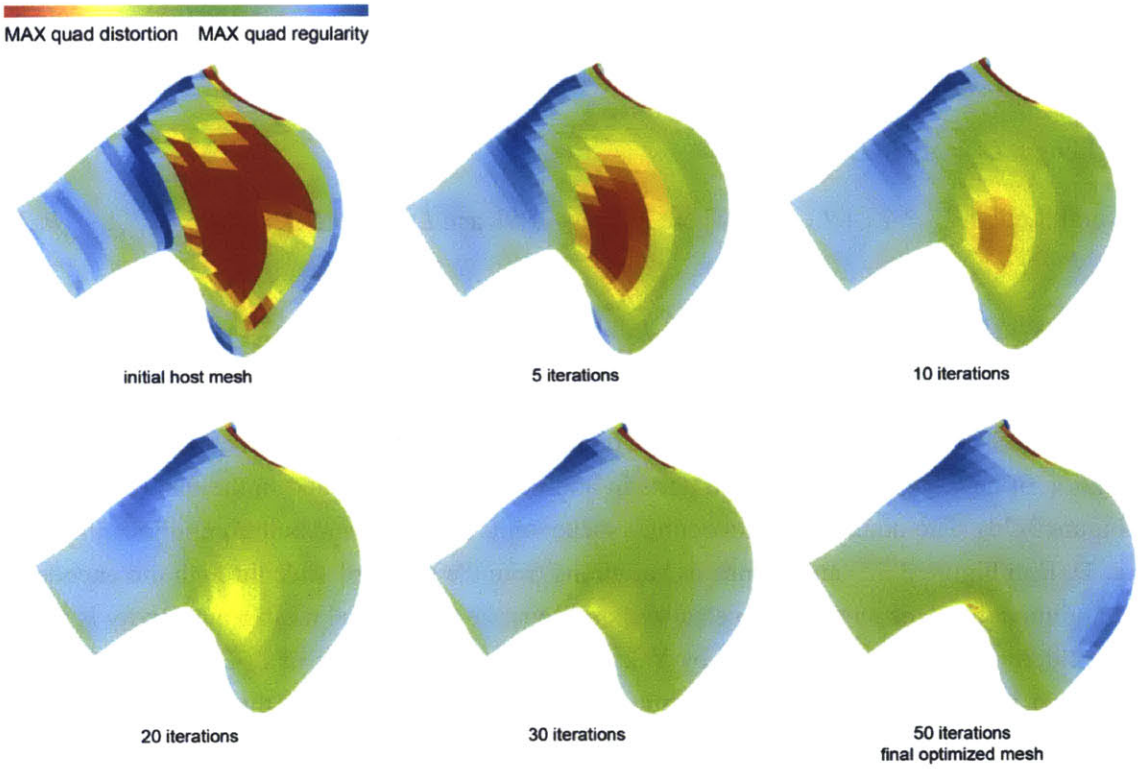

Figure 3-10: STP global iterative steps for regularizing the host mesh Tangential Laplacian Smoothing through 50 iterations. The quality of the quad ranges from distorted (red) to regular (blue). Figure from Duro-Royo et al. [2014b].

with lowest values of FC in the upper arm area and highest values in the underarm. This step demonstrates a generative framework for computationally mapping segmented unit geometries to a complex surface while future iterations of the model will implement physiological data for human joints (Duro-Royo et al. [2014b]).

A global mesh optimization strategy is then applied as illustrated in Figure 3-10. The Tangential Laplacian Smoothing algorithm regularizes the hosting mesh geometry by iteratively repositioning the mesh vertices according to the geometries dictated by the FC without distorting the overall shape of the mesh. A homogenization optimization algorithm is applied to the hosting mesh. The rational behind optimizing for homogeneity is to avoid local spatial heterogeneities and discontinuous changes in the composite structure that would result in stress concentrations, weakened areas and might lead to buckling or kinking, and discomfort by the wearer. This algorithm maximizes the homogeneity across all of the quads in the mesh by replacing each vertex coordinate with a weighted average of itself and its first order neighbors (Zhang et al. [2005]). In the model, a vertex displacement vector x_i is calculated for each vertex $x_i : xi = 1nij\varepsilon v_i = x_j - x_i$. Vertex displacements are then applied to the vertex coordinates, $x_i' = x_i + \lambda xi$, where λ is a fixed-scale parameter in the range 0 $< \lambda < 1$. Finally, I replace the original vertex coordinates X with the new vertex coordinates X' (Taubin [2012]).

These three steps are repeated until maximum quad homogeneity for minimum unit distortion is

achieved. Here, it is important to preserve the shape of the mesh as new vertex positions are applied; the model avoids mesh shrinkage by limiting vertex translation as only tangential to the mesh surface. Figure 3-10 demonstrates the iterative steps for regularizing the host mesh Tangential Laplacian Smoothing through 50 iterations, while the quality of the quad ranges from distorted (red) to regular (blue). Future modification to this optimization algorithm seek to fit vertex relocation to physiological data for joint flexure, assign internal porosity to minimize weight, or distribute multiple materials for tunable composite structures with desired mechanical properties (Duro-Royo et al. [2014b]).

Translation to Human Mesh: I validate the STP computational modeling process by using it to populate a host mesh of a human shoulder with protective scales. Figure 3-12 presents an overview of this process. A regular polygonal mesh of quads with boundaries is optimized from a distorted base mesh of a human shoulder. A regional directionality pattern is applied over the mesh edges to inform the construction of scale connectivity. The functional gradient is then determined according to an estimate of human biomechanics and applied to the mesh vertices. Finally, the units are adapted to the smoothed geometry through integration of neighborhood parameters encoded into the mesh vertices for each scale. The association of the local unit parameters to its neighbors in addition to the underlying mesh information (FC and regional directionality) allows for the computational translation of the segmented assembly of units adapted to the host geometry while preserving articulating connections between the units. The current composite exoskeleton design is materials-generic and allows for the fabrication of varied exoskeletons composed of arbitrary choice of structural materials. The weight of the exoskeleton is driven by the material choice for the rigid individual armor units and related to the composite volume fraction (volume of rigid armor units Va / volume of organic Vo). Volume fraction is calculated at various locations of the exoskeleton in the model and found them to be in the 1.5-1.7 range (Duro-Royo et al. [2014b]).

3.3.4 STP Discussion

The STP model is a generative computational design workflow for translating design principles observed in the flexible fish exoskeleton of P. senegalus into functionally graded structures adapted to a new host surface, e.g. a human shoulder. Figure 3-12 summarizes the main steps in translational process from analysis of the biological armor into generative computation through local shape construction, regional connectivity pattern, and global optimization and adaptation to overall geometry. STP attempts to solve many challenges heretofore unaddressed in architectural geometric design and flexible protective structures by developing bio-inspired functional designs with components operating at multiple length scales (Duro-Royo et al. [2014b]).

The originality of STP lies in its efficient workflow linking experimental analytical methods (uCT and morphometric analysis) with advanced computational geometry techniques (custom data structures for polygon mesh processing and component adaptation). The results propose a novel strategy for the multifunctional adaptation (Figure 3-11a, Figure 3-11b) of highly elaborate components to complex surfaces with tailored directionality, emergence of new unit types, and the conservation

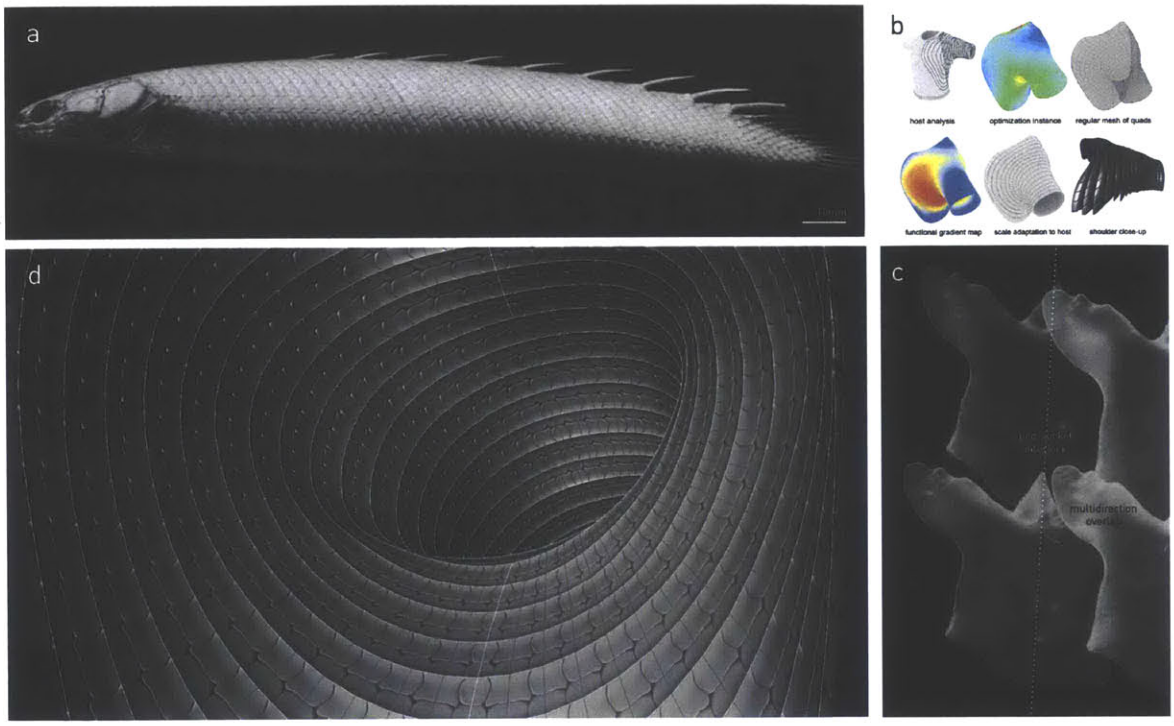

Figure 3-11: (a) Translation of armor system from prehistoric fish P. senegalus. (b) Iterative computational model for multifunctional adaptation of highly elaborate components to complex surfaces. (c) Interconnectivity patterns of interlock and overlap. (d) Visualization of the fish armor translated into a human body shoulder and arm.

of their interconnectivity patterns (Figure 3-11c, Figure 3-11d). Furthermore, the computational model sets the basis for future work with different exoskeleton systems and for the optimization of requirements beyond the topology of the hosting surface, such as kinematic ranges of motion, porosity for breathability requirements, or material distribution within units to modulate materials and mechanical properties in various regions (Duro-Royo et al. [2014b]).

3.3.5 STP Model Results

Customized computational models like STP provide a novel and effective method for translating the intricate, multifunctional design principles found in natural structures such as mineralized exoskeletons to synthetic, bio-inspired structures. These models challenge traditional CAD-based design techniques and set the basis for the incorporation of multiple layers of information, such as physiological and kinetic dimensions, at any level of the hierarchical computational data structure, importantly pointing towards a new design workflow characteristic of Fabrication Information Modeling (FIM).

STP is a computational model that embeds the geometric complexity of mineralized exoskeletons to enable functional gradation to the new bearer. The customized data structure provides adaptation of the system, while varying the unit features with neighborhood connectivity ensures graded overlap and interlock. With the STP model it is now possible to encode hierarchical relationships at local, regional, and global levels to maintain complex connectivity and functional differentiation of

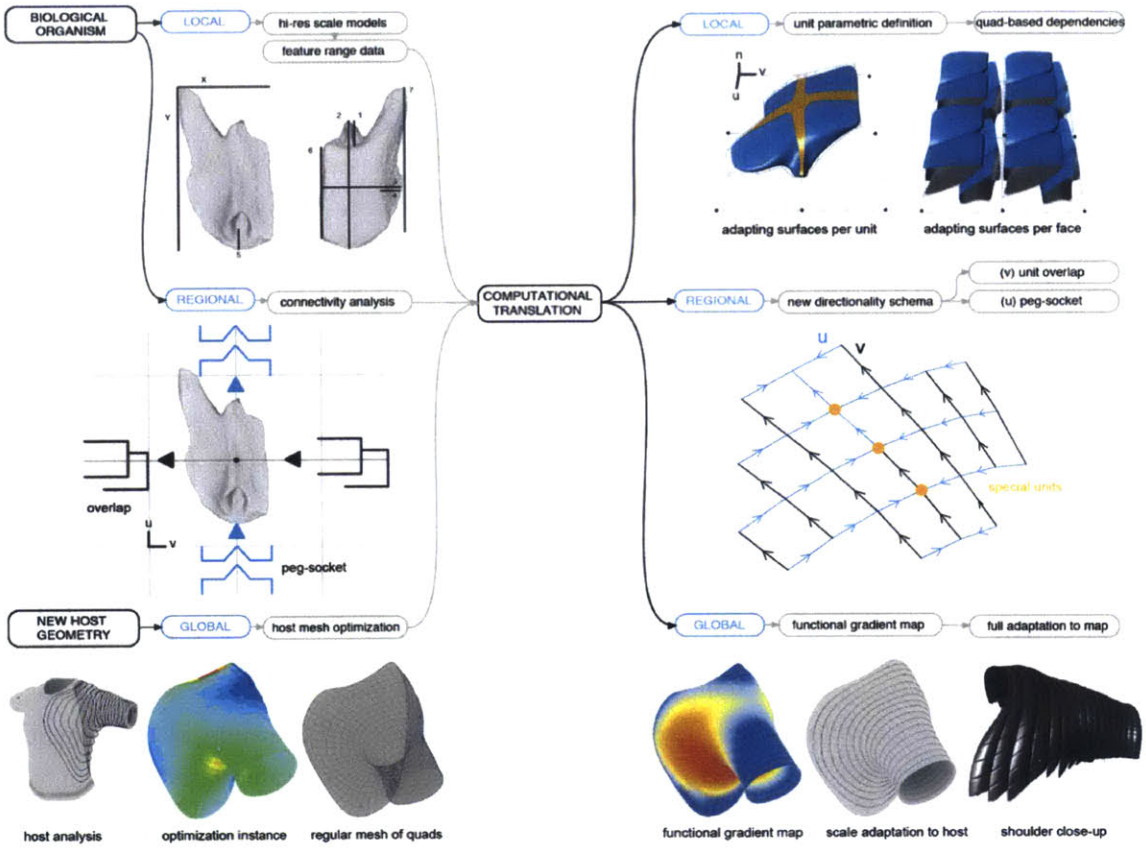

Figure 3-12: Graphical summary of the STP hierarchical computational model. Figure from Duro-Royo et al. [2014b].

articulated structures on complex hosting surfaces (Duro-Royo et al. [2014b]).
Through STP, interdisciplinary research (here drawing on experimental biology, materials science and engineering, mechanical engineering, and architecture) contributes to a better understanding of biological design principles and enhanced translation to bio-inspired and biomimetic devices. Scientific perspectives on the geometric and materials analysis in the P. senegalus exoskeleton better inform the designer in devising computational methods to translate designs to a new hosting surface and fabricate a functional bio-inspired system (Duro-Royo et al. [2014b]).

3.4 Environmentally driven Swarm Printing System (SPS)

The SPS model is implemented for a distributed approach to construction of larger-than-gantry size structures exhibited at the Lisbon Architecture Triennial 2014. A multi agent system is developed composed of cable-driven robots ("cable-bots") able to deposit material drops in a layered manner. Material curing times are computed in the system along with swarm-like motion behavior rules of space exploration. Structural emergence is achieved with only punctual designer's input opening up approaches for long distance fabrication (Figure 3-1c) (Duro-Royo et al. [2015b]) (more information on the computational model can be found in DuroRoyo et al. [2015]). Mechanic development of the system is implemented with Markus Kayser and Jared Laucks, and electronic and software development is achieved in collaboration with Laia Mogas-Soldevila.

3.4.1 SPS Digital Implementation Details

Software: The distributed system is implemented in a Java language customized applet enabling real-time 3D representation of the agents' behavior. There are two sets of functionalities in the applet relating to two modes, the setup mode and the building mode. The setup mode takes as input data each agent's envelope dimensions and base. The envelope dimensions of each agent are measured in 3D physical space, where the top corners of each envelope are placed parallel to the construction base plane. The agent's base is an origin point measured in space where the robot builder is at rest. With this information at hand the system is able to determine initial cable lengths and to reset motor encoders as a starting point for subsequent construction behavior. Figure 3-15 shows the setup interface where initial data is read from motor encoders, and then used to position extruder head as well as to test the extrusion stepper motors.
The building mode function calculates the trajectories and temporal positions of each agent employing linear trajectories and constant velocity. I use a 3D modification of the Bresenham algorithm (Bresenham [1965]) to move and track the agents in space via shortening or lengthening one of the four cables that are assigned per agent. The system computes discrete close approximations to linear trajectories from any 3D origin to any 3D target in the agent's envelope. Trajectory corrections are applied to avoid collision although agent envelopes may overlap, allowing for co-construction in specific and designated areas (DuroRoyo et al. [2015]).

3.4.2 SPS Mechanics and Materials Details

Mechanical Assembly: Machine control firmware is developed in C and C++ language using micro controller boards (Arduino Mega 2560). The boards distribute serial signals to stepper motors (Gecko 6723-400-4) via the Probotix Bi-polar 7.8A drivers. The motors are NEMA 23 in size and are rated for a holding torque of 2.83 newton-meter. The drivers permit a maximum current of 7.8A and are powered separately from the electronic controls with a 48V power supply. Constant force spring motor assemblies (Stock Drive Products/Sterling Instruments, ML 2918) are used to spool up excess cable as well to keep tension on the pulleys. The micro controller receives feedback data from incremental rotary encoders (Yumo, A6B2-CWZ3E-1024, 1024 P/R Quadrature) and custom made zero switches comprised of copper contact and a connecting copper element attached to the cable at the right length. Each agent is suspended via four straight center stainless steel cables which are encased in a helically wound nylon/polyurethane sleeve (Stock Drive Products/Sterling Instruments, Synchromesh, 1.6mm outer diam.). Each custom-built extrusion head assembly is composed of a stepper motor with a rubber seal and a custom extrusion screw. Lead weights are applied for stabilization of the extruder head; cable fixtures are attached to four incoming cables with machined plastic housing and a material supply inlet Figure 3-14. The material feed for each head is composed of a pressure pot containing paste-like material fed to the extrusion heads by narrowing the flexible tubing diameter towards the extrusion head Figure 3-14 (DuroRoyo et al. [2015]).

3.4.3 SPS Environmentally driven Swarm Printing System

Distributed Construction Background: The majority of current research efforts in distributed construction focus on the assembly of discrete components (e.g. blocks or beams) held together in ways that are not readily scalable (e.g. magnetism or friction) (Lindsey et al. [2011], Werfel et al. [2014]). These systems are typically developed around specific modular or prefabricated components, which limit the range of possible geometries and applications of the resulting structure (Lindsey et al. [2011], Werfel et al. [2014]). From a design perspective, such efforts focus either on duplicating existing rectilinear forms as made by conventional construction methods (Lindsey et al. [2011]), or on simulation models that fail to be reproduced in physical environments (Tan and Zheng [2013]). Few recent projects, such as the one presented here, explore distributed deposition of large-scale structures with tunable material properties (Naboni and Paoletti [2015], DuroRoyo et al. [2015]).

Additive Manufacturing Background: Current additive fabrication approaches for digital construction are generally limited by 3 major constraints: (1) the typical use of non-structural materials with homogeneous properties; (2) the dependency of product size in the gantry size, and; (3) the typical need for support material throughout the layered deposition process (Augugliaro et al. [2014], Naboni and Paoletti [2015], Oxman et al. [2014]). A distributed approach to manufacturing carries potential to radically transform digital construction by (1) digitally fabricating structural

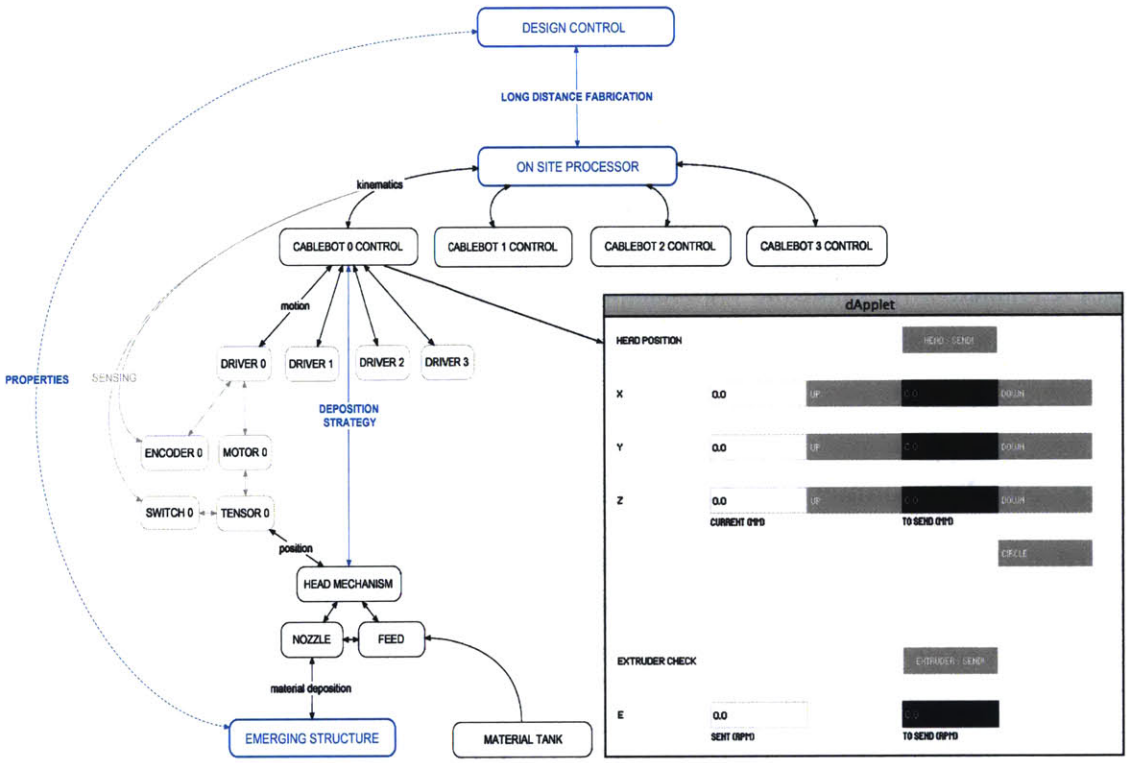

Figure 3-13: Flowchart and applet setup mode interface capture of the virtual implementation of a large-scale distributed cable-suspended additive construction platform. Figure from DuroRoyo et al. [2015].

materials with heterogeneous properties (Oxman et al. [2012]); (2) generating products and objects larger than their gantry size (Oxman et al. [2014]); and (3) supporting non-layered construction by offering novel fabrication processes such as free-form printing and robotic weaving (Oxman et al. [2013b, 2014]). Building on the previous work, a work-in-progress distributed multi-robot approach to additive construction at architectural scales is proposed (DuroRoyo et al. [2015]). Interesting design opportunities emerge when more than a single material deposition node shares a construction space. The implications of robotic collaboration are vast and must relate to challenges such as agent awareness to boundary condition, envelope sharing across agents, real time multi-agent 3D positioning protocols, means for collision avoidance, and distributed preservation of the mechanical cable-suspended system as well as the material deposition feed (DuroRoyo et al. [2015]).

Main rule set: The main computational rule set encodes five key system functions. Those include three centralized operations - avoidance, storing and linking, and two decentralized operations - search and deposition. The avoidance function (1) keeps track of each robot's position in space in order to avoid cable hyperextension when agent navigation occurs outside the determined envelope. It also supports collision avoidance either by pausing one of the agents or by modifying its trajectory. The storing function (2) saves the position and deposition time of each drop of matter placed onto the structure. The linking function (3) ties the emergent structure with design intent rules such that the designer can steer the robots towards building in certain areas and avoiding others. This is achieved by operating the virtual tool through a representation of the physical structure as it is being collaboratively built Figure 3-15 (DuroRoyo et al. [2015]).
Included in the decentralized operations, is the search function (4) designed to enable the agents to explore their envelope spaces and determine an adequate deposition location. During search mode, the robots navigate in 3D by employing bouncing trajectories from their maximum envelope until a z-axis threshold is trespassed; then, the agents verify the possibility of depositing material with the central system. Given a 3D position for additional material - if the relative height of the neighboring structure and the curing time of the underlying drops are adequate - a new drop will be deposited. During the construction phase, the z-axis threshold is modified in order to adapt to the current height of the construction. Finally, the depositing function (5) consists simply of depositing a material droplet in a specific position as well as relaying time and coordinates to the central system (DuroRoyo et al. [2015]).

Adaptation to material conditions: Material deposition is informed by data embedded in the material itself. Each time a droplet of matter is deposited by a cable-robot agent in the physical environment, the virtual central system stores its data in a clock-based counter. The next agent attempting to deposit a new droplet on top of the stored one, receives information about the structural properties of the existing construct based on expected curing times. If the curing time is adequate, the agent will deposit a new droplet on top of the structure. Else the agent will enter search mode and determine an alternative spot to deposit the stored material. Preliminary results demonstrate small-scale proof-of-concept of structural organization of droplets and proper discrete material bonding. Figure 3-16 (top) shows first construction results of a layer of 14 inch diameter droplets by one of

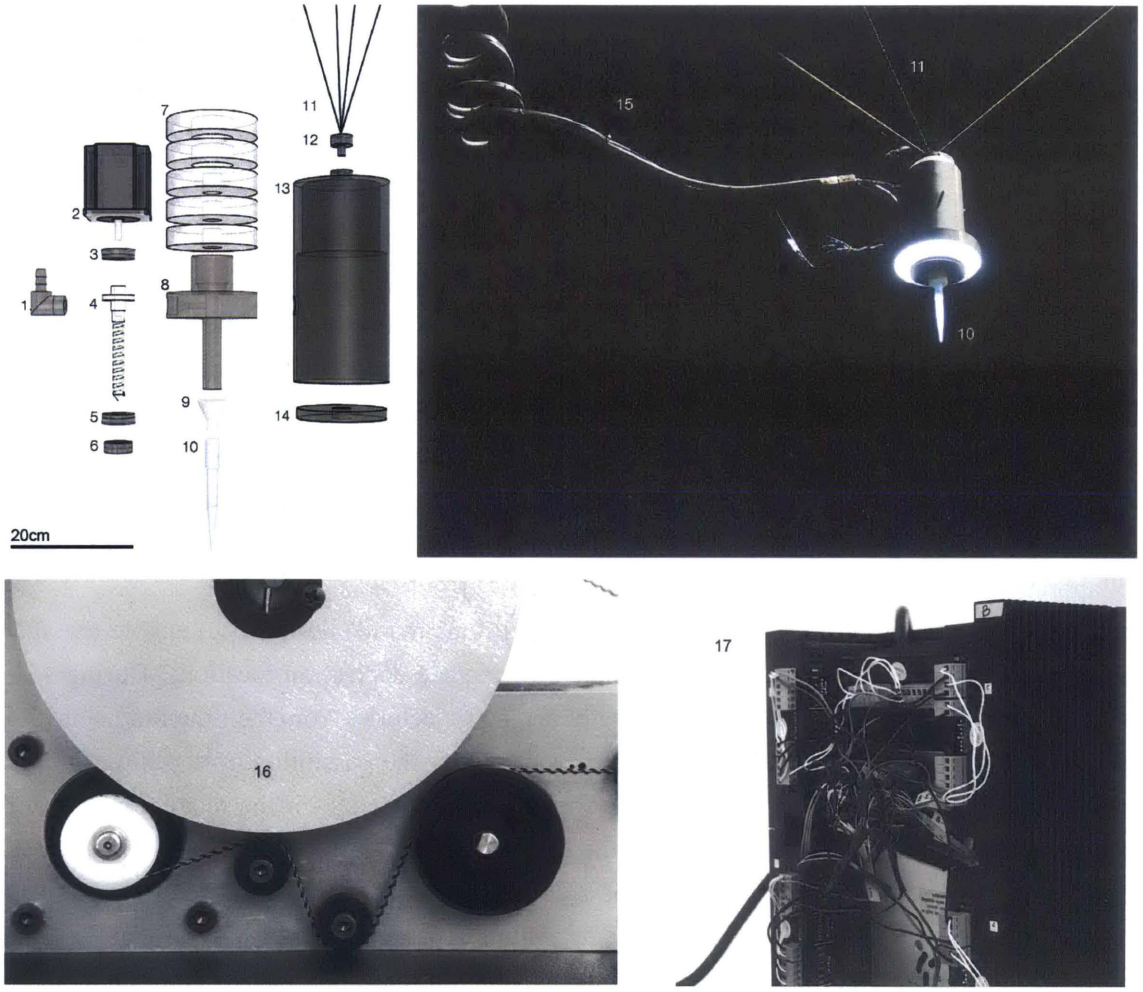

Figure 3-14: Electro-mechanical implementation for a cable-suspended construction system. The extruder head assembly is composed of material inlet (1), stepper motor (2), rubber seal (3), custom screw (4), rubber seal (5), U seal (6), lead weights (7), screw mixing chamber (8), HDPE custom nozzle (9), pipette tip (10), synchromesh cable (11), cable fixture (12), delrin housing (13), and end cap (14). Material is fed via hierarchical tubing (15). Spring motor assembly for synchromesh cable (16), and electronic control assembly (17). Figure from DuroRoyo et al. [2015].

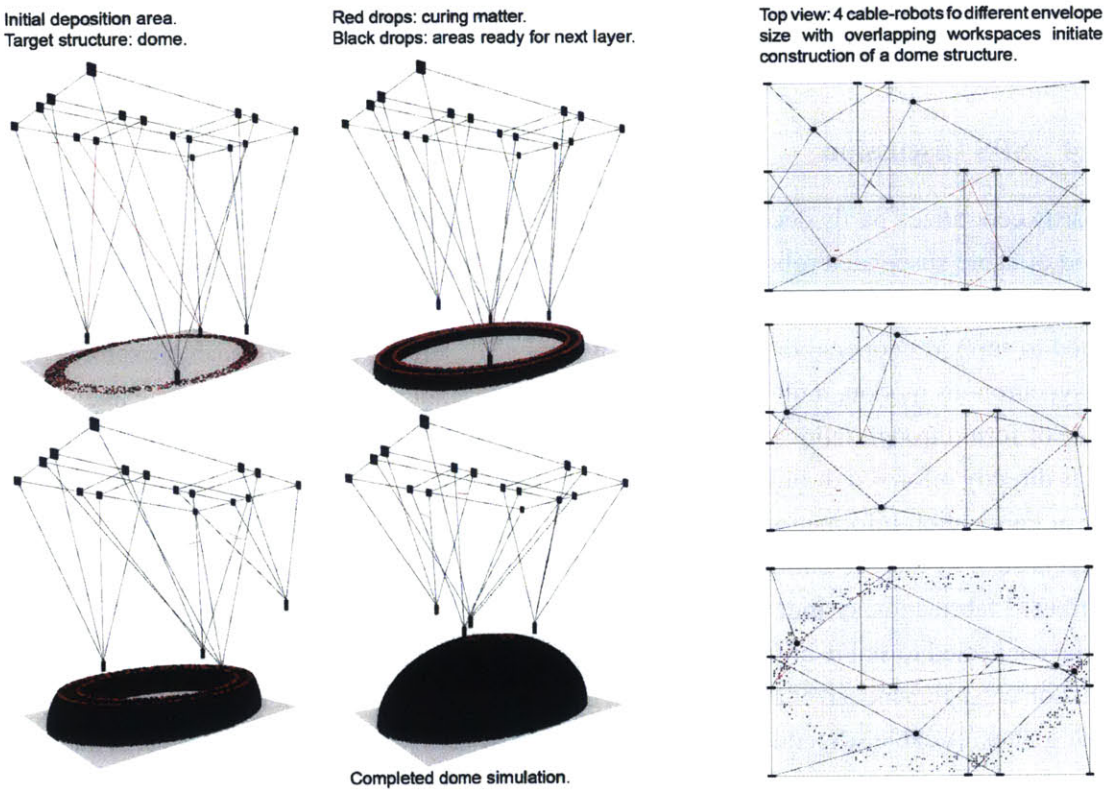

Figure 3-15: Virtual simulation of a cable-suspended construction system. Robot envelopes are differently shaped and overlap with each other in order to collaboratively build a structure that is bigger than each individual machine's gantry. Figure from DuroRoyo et al. [2015].

the cable-robot extruders performing rule-based search motion in between depositions. Different droplet-based typology configurations have been tested by manually directing an extruder to pre-set positions namely; 4-faced vault, nave, discontinuous wall, and cantilevered continuous wall Figure 3-16 (bottom). The material system used is industrial soft putty filler paste composed of gypsum plaster from hydrated calcium sulphate and glue. The virtual and physical systems are currently ready for the implementation of real-time feedback using humidity sensors or thermal cameras reporting to the central program (DuroRoyo et al. [2015]).

Adaptation to design intent: The construction strategy presented here complies with global electro-mechanical constraints in a rule-based system for the generation of form, while maintaining an adaptation strategy for direct remote intervention. The designer sets up the system to build a structural typology (e.g. a dome, an arch, a column array etc.), and lets the behavioral model initiate its construction in a bottom-up manner. The cable-robots negotiate the construction space without top-down specifications for which agent will build what section of the structure. However, in case of local structural instability or in case of design iteration during the building sequence, the designer can steer the agents toward abandoning an area or focus on completing another. This technique enables the emergence of form through robotic node-to-node communication by applying space negotiation rules for each drop deposition. Exploration of this feature is not possible with

continuous layering of material employed in traditional 3D-printing extrusion technologies, such as fused deposition modeling (FDM) (Oxman et al. [2014], DuroRoyo et al. [2015]).

3.4.4 SPS Discussion

A partly centralized partly decentralized digital fabrication environment is designed and build composed of cable-suspended robots. This environment demonstrates the first steps towards the design and construction of a novel fabrication technology made up of multiple fabrication nodes that is designed to support cooperative construction of large-scale structures. The research explores themes of asynchronous motion, multi-nodal fabrication, lightweight additive manufacturing and the emergence of form through fabrication. Importantly, the project points towards a new design workflow that is directly informed through fabrication, material and environmental constraints, and characteristic of Fabrication Information Modeling (FIM) (DuroRoyo et al. [2015]).
Systems such as the one outlined here can be deployed for large-scale construction by attaching a distributed fabrication system to existing objects in the built environment. Cables from each robot can be connected to stable high points, such as large trees or buildings (Oxman et al. [2014]). Such actuation arrangement can enable movement over large distances without the need for conventional linear guides. A cable suspended system is straightforward to set up for mobile projects and affords sufficient printing resolution and build volumes (DuroRoyo et al. [2015]).

3.4.5 SPS Model Results

Distributed forms of construction in the biological world are characterized by the ability to generate complex adaptable large-scale structures with tunable properties. In contrast, state-of-the-art digital construction platforms in design lack such abilities. This is mainly due to limitations associated with fixed and inflexible gantry sizes as well as challenges associated with achieving additively manufacturing constructs that are at once structurally sound and materially tunable. To tackle these challenges a multi-nodal distributed construction approach is proposed that can enable design and construction of larger-than-gantry-size structures (DuroRoyo et al. [2015]).
The system can generate and respond to integrated real-time feedback for parameters such as material curing duration and position awareness. I demonstrate this approach through a software environment designed to control multiple robots operating collaboratively to additively manufacture large-scale structures. The environment combines a centralized system designed to manage top-down design intent given by environmental variables, with a decentralized system designed to compute, in a bottom up manner, parameters such as multi-node rule-based collision, asynchronous motion, multi-nodal construction sequence and variable material deposition properties. This approach points towards characteristics of the Fabrication Information Modeling (FIM) approach. This reports on a successful first deployment of the system and demonstrates novel features characteristic of fabrication-information modeling such as multi-nodal cooperation, material-based flow and deposition, and environmentally informed digital construction (DuroRoyo et al. [2015]).

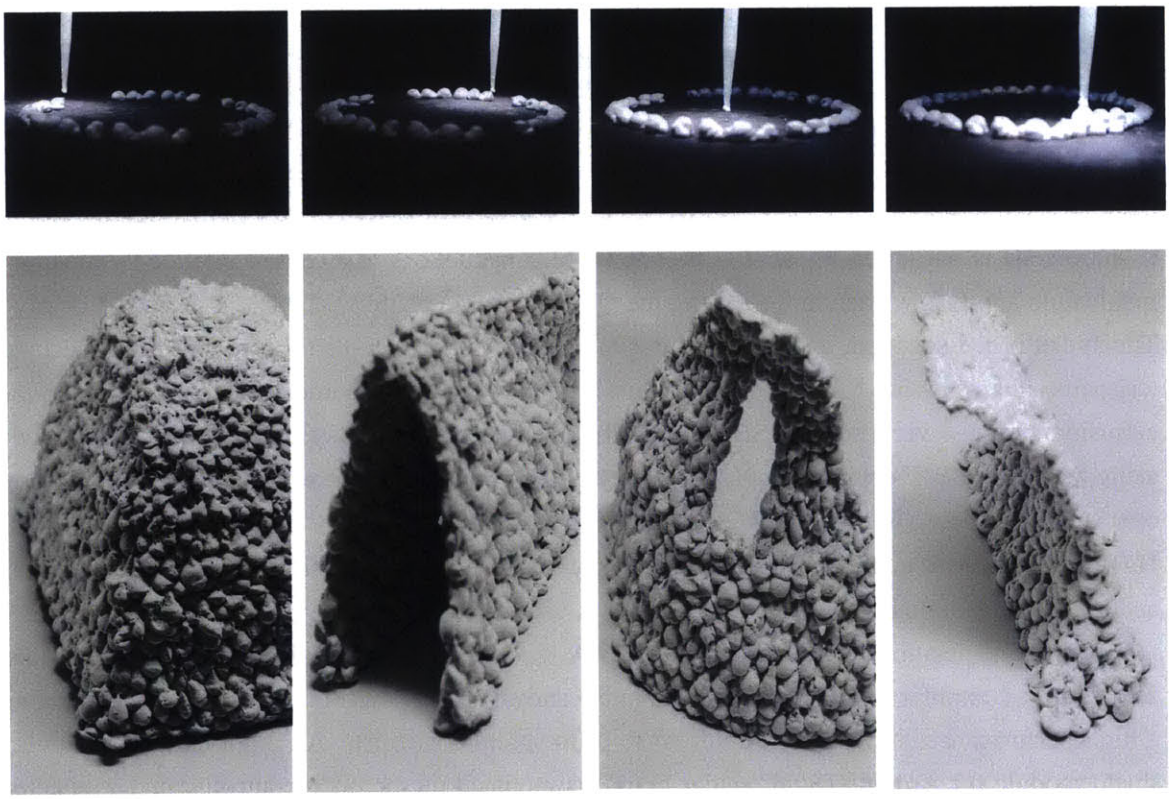

Figure 3-16: Top: Initial results of robotic deposition of layered droplets performed by one cable-robot extruder. Bottom: Preliminary manual experiments in soft plaster deposition including a 4-faced vault, a nave, a discontinuous wall, and a cantilevered continuous wall performed by Laia Mogas-Soldevila. Figure from DuroRoyo et al. [2015].

3.5 Manufacturing-driven Hierarchical Fabrication Platform (HFP)

In the HFP model the goal is to design and fabricate large-scale biomaterial structures. I implement a customized computational workflow integrating multi-scale material distribution. The material micro-to-macro distributions respond to deposition of hydro-gels with variable mechanical properties in single or multiple layers. The final designs demonstrate emergent geometries and are fabricated with a customized material deposition platform (a portable customized multi-nozzle deposition tool attached to an industrial Kuka KR robotic arm) (Figure 3-1d) (more information on the computational model can be found in Duro-Royo et al. [2015a,b]).

3.5.1 HFP Digital Implementation Details

Software: Geometric objects and tool paths presented here are designed within the Rhino3D modeling software environment (2013, Rhinoceros, Robert McNeel and Associates, USA) and its scripting plugin, Grasshopper (McNeel [2010]). Using the geometric kernel library of the plugin, custom C-sharp code is written to transmit fabrication XML instructions to a central interface. The communication applet is written in C++ using the Qt open-source platform (2014, Qt project, Norway). The applet processes input and output data generated in the design platform to and from mechanical parts. Transmission to the motion system is achieved via an Ethernet UDP socket, and to the extrusion system - via a serial USB signal. The pneumatic tool firmware is developed in C code using the Eclipse IDE environment (2014, The Eclipse Foundation, Canada) and the cross-platform open-source Arduino library (2014, Arduino Software, Italy).

Hardware: A Mastech Linear DC power supply, model 30V 5A HY3005F-3, with triple outputs and dual adjustable outputs (0-30V and 0-5A) is used to power pneumatic hardware components for positive and negative pressure at 25V and 0.6A. The system's control board is an Arduino Mega 2560, with a computer supplied input power of 5V and an output power of 3.3V or 5V, incorporating a high performance, low power Atmel AVR 8-Bit micro-controller. An eight-channel 5V relay shield module for Arduino (SunFounder brand) is mounted on the microcontroller and connected to positive and negative pressures. Pressure is controlled by directional solenoid valves with a 3-way, 2-position, normally closed spring return poppet valve with aluminum stackable body. Other valve specification include: 1/8 inch NPT female ports, Cv=0.051, 24VDC single solenoid, 11mm DIN style wiring connector, and a minimum response time of 0.05s, which I take into account in the computation sequence. Pressure is tuned with a compact size general-purpose electronic pressure regulator, converting a 4 to 20 mA signal to a proportional pneumatic output (ranging from 0 to 120PSI) with a sensitivity of 2.5% of span per PSI (OMEGA IP610-X120). I included a 1s response time for the regulator. Signal to the regulator is computed through a low-power high-accuracy single channel, 12-bit buffered voltage output Digital-to-Analog Convertor (DAC) board with non-volatile memory (MCP4725 Board). Output pressure from the regulator is read with a ProSense digital pneumatic pressure transmitter, with a -14.5 to 14.5 psi range, 2 PNP, 4-20 mA, 1/8 inch NPT outer pressure connection, M5 inner pressure connection, powered by 12-24 VDC.

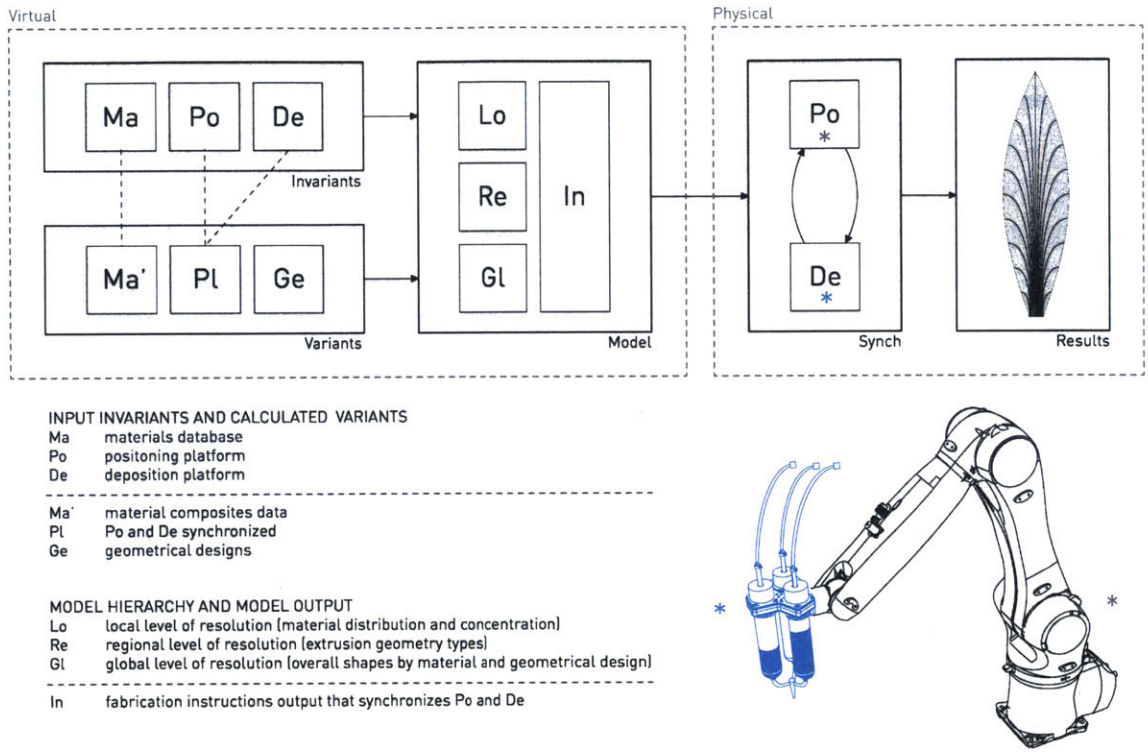

Figure 3-17: Overview of the computational workflow for design and direct additive manufacturing of heterogeneously structured objects. Virtual hierarchical computation is implemented at local (Lo), regional (Re) and global (Go) levels of organization. It combines variants and invariants given by base materials (Ma) and their combinations (Ma'), the positioning platform (Po), the deposition platform (De) and the geometrical design (Ge). The model generates fabrication instructions (In) that are transmitted in synchrony to both platforms (Pl). Heterogeneous structured results are obtained from this seamless virtual-to-physical workflow. As an example, a positioning platform (Po) is depicted as a 6-axes robotic arm and a deposition platform (De) is depicted as a three-barrel pneumatic extruder. Figure from Duro-Royo et al. [2015a].

The hardware assembly detailed here is illustrated in Figure 3-17b).

3.5.2 HFP Mechanics and Materials Details

Mechanical Assembly: The extrusion system is attached to an existing motion platform's end-effector. The platform is a Kuka KR AGILUS robotic arm; model KR 10 R1100 SIXX WP. It weighs 54kg with a 10kg payload and a maximum reach of 1101mm. It has 6 axes, a +-0.03mm repeatability and employs the KR C4 compact control system. At the pneumatic extrusion end-effector, different materials are contained in six 300cc clear plastic dispensing syringe barrels with hard rubber plungers, and extruded with 7mm and 2mm customized HDPE plastic nozzles. Flow valves, gauges and tubing are dimensioned to 4mm 10PSI to 120PSI pneumatic circuitry. Positive pressure is obtained with a 4.6 gallon aluminum twin-tank air compressor with 1.5 horsepower, 120 volts, 60 Hz 4.2 CFM at 90 PSI and 5.4 CFM at 40 PSI. Negative pressure is obtained with a rotary vacuum pump at 1725 RMP and 110 volts, 60 Hz. For the mounting of the custom end-effector parts we used 5mm and 10mm machinable aluminum sheets cut with a numeric control abrasive

water-jet machine (OMAX Corporation, USA). These mechanical assembly parts are illustrated in Figure 3-19b (Duro-Royo et al. [2015a]).

Deposition Materials : The multi-material pneumatic deposition tool-head that is developed is able to extrude materials with viscosities ranging from 500cPs to 50.000cPs at room temperature such as; hydrogels, gel-based composites, certain types of clays, organic pastes, resins, polyvinyl alcohols etc. In the experiments presented here polysaccharide hydrogels are used in 1% to 12% concentrations in w/v of 1% acetic acid aqueous solutions, as well as these gels mixed with cellulose microfiber to obtain volumetric composites. Their testing, characterization and processing are explained in detail in the previous publication (Mogas-Soldevila et al. [2014]) and in the patent (Duro-Royo et al. [2014a]). The materials present visco-plastic or visco-elastic behaviors inside airtight barrels and undergo slow curing from pastes to solids at room temperature. Exhaustive empirical testing of these materials and their combinations is stored in the platform's database to inform calculations of the model's parameters for pneumatic deposition and positioning motion. Other synthetic materials such as fuse deposition manufacturing (FDM) polymers can be used as well, by implementing heating nozzles, as material and tool settings are externalized from the core computation (Duro-Royo et al. [2015a]).

3.5.3 HFP Manufacturing-driven Hierarchical Fabrication Platform

I present a model, an enabling technology and a workflow sufficiently generalized to adapt to a wide range of materials and digital fabrication platforms (Duro-Royo et al. [2014a]). The proposed workflow is designed to integrate the virtual modeling environment to the physical fabrication platform, achieving multi-material and multi-property constructs at the service of multi-functional objects (Figure 3-17). I propose that seamless computational workflows such as the one presented here, can be viewed as vehicles to encode multidisciplinary non-standard design constraints into generative frameworks. These frameworks can provide for methodological design tools that enable navigation between tightly related constraints typical of complex and heterogeneous designs (Duro-Royo et al. [2015a]).

Every flow layer included in the system is independently defined. Importantly, 3D constructs characterized by complex material organization will emerge, not by direct 3D modeling, but by meta-data instructions informing the manufacturing process through variable motion speed, variable pressures and diverse water-based viscous material compositions. These interrelated processes can be rationalized through domain-specific flow fields. Flow fields include the flow of data, the flow of bits, the flow of motion, the flow of pressure, the flow of time, and the flow of water.

The Flow of Data : The flow of data is initiated by variant design parameters and invariant system constraints defined by the system's building blocks. These include: the materials to be extruded (Ma, Ma'), the positioning platform (Po), the deposition platform (De), and the geometrical designs (Ge) (Figure 3-17). The system is defined in a way that is as general as possible by variant and invariant constraint parameters independent and external to the hardware system in use. The goal is to enable its implementation using various DDM platforms. In the current testing system a posi-

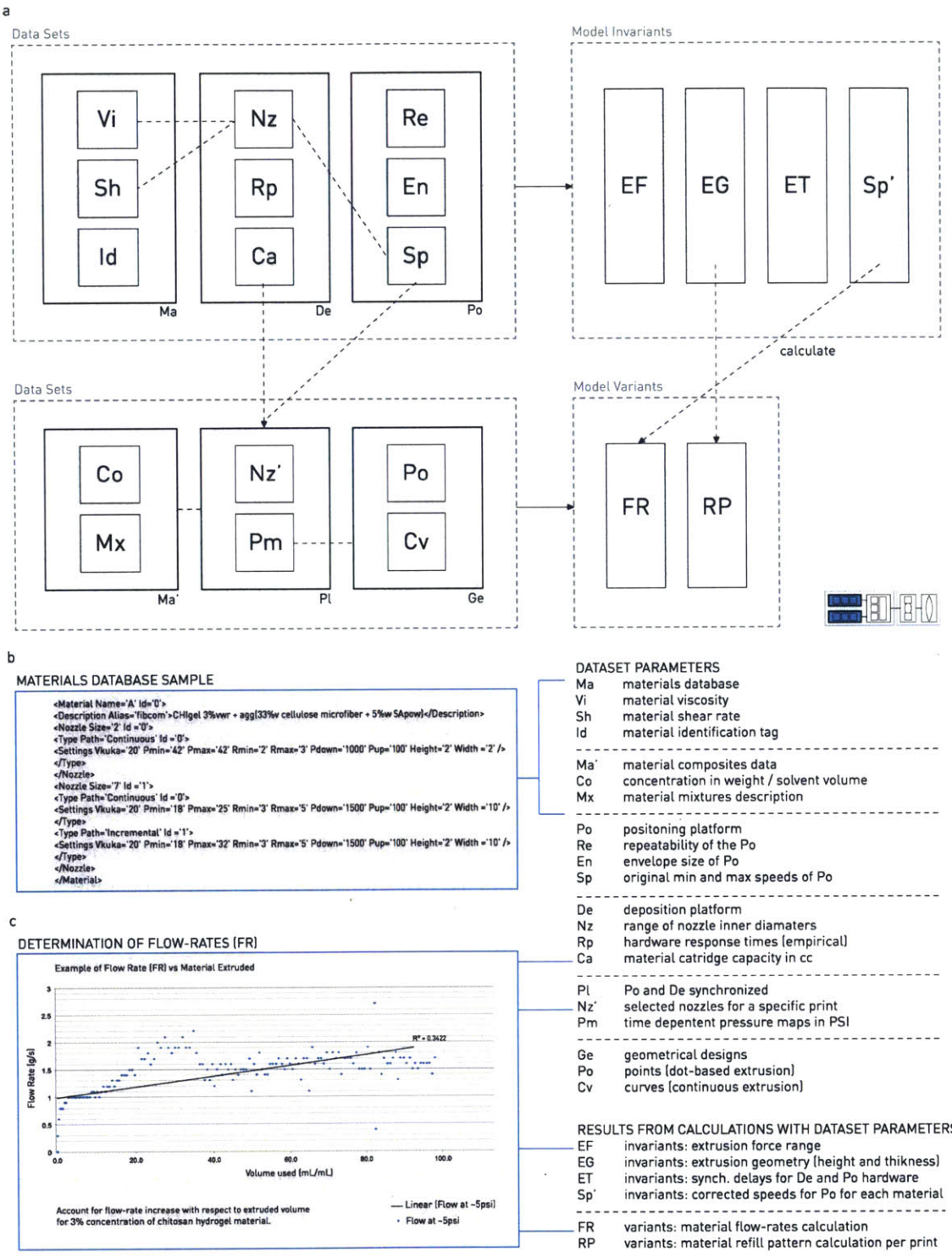

Figure 3-18: (a) Data including materials (Ma, Ma'), platform parameters (Po, De, Pl), and geometrical design (Ge), is incorporated within the computational model. Processing of this data into calculations results in global constants (invariants) and design specific parameters (variants). The model invariants compute the range of extrusion forces (EF), the height and thickness ranges of the extrusion geometries (EG), the extrusion delays and synchronization timings required (ET), and the corrected speeds of the positioning platform (Sp'). The model variants compute the required flow-rates (FR), and the pattern of barrel refills over time (RP). (b) A sample of the materials database. Empirically tested material specific parameters such as minimum and maximum extrusion pressure, nozzle height, hardware delays, and motion speed are stored and used for the calculation of code variants. (c) Corrections are added to the extrusion pressure calculation by determining the linear increase of flow-rate due to cartridge level changes over time. Figure from Duro-Royo et al. [2015a].

tioning platform (Po) is given as a 6-axis robotic arm, and a deposition platform (De) is given as a multi-barrel pneumatic extruder (Figure 3-17, Figure 3-19) (Duro-Royo et al. [2015a]).

Invariants : Invariant constraints serve to calculate the platform-specific constant parameters of the system. Parameters related to base materials (Ma) include: viscosity (Vi), shear rate (Sh) and material identification (Id). I calculate the invariant constraints of the deposition platform (De) through: range of nozzle types (Nz), hardware response times (Rp), and material reservoirs capacity (Ca). Previous research into nozzle designs can be found in (Mogas-Soldevila et al. [2014]) (Figure 3-18a).
Finally, the invariant constraints of the positioning platform (Po) are calculated using: system repeatability (Re), envelope size (En), as well as minimum and maximum speeds (Sp). With the mentioned sets of parameters, the system can calculate the invariants which are: range of extrusion forces (EF) required for a given design, the range of extrusion 3D-shapes to be deposited (EG), the range of extrusion timings and delays, and the revised speeds (Sp') of the positioning platform (Figure 3-18a) (Duro-Royo et al. [2015a]).

Variants : Variant constraints serve to calculate specific parameters of the computation that change at every design. They relate to parameters from the selection and combination of base materials (Ma) into composites (Ma'); degree of concentration of material in solvent (Co), and description of the composite characterization for further reference and testing (Mx) (Figure 3-18b). A calibration capability can be used such that, in addition to the set of initial materials (Ma), an extendable database of material behavior is stored as different materials are tested by the system. This practice allows for platform and workflow validation at step of the development process (Duro-Royo et al. [2015a]).
Other platform parameters available that contribute to variant calculation include: nozzle type chosen (Nz') e.g. to perform co-axial, parallel or mixed extrusions as well as time-dependent pressure maps (Pm) that determine the extrusion geometry. Hardware response times (Rp) are calculated empirically and inform the calculations, as well as the measurements of the cartridge capacity (Ca). Continuous, discontinuous or discrete geometries, such as points (Po) or curves (Cv) can be assigned with the aforementioned material choices and time-dependent pressure maps. With the mentioned sets of parameters, the system is designed to calculate the range of variant flow-rates (FR) required for a particular multi-material design, and patterns of reservoir refill over time (RP) (Figure 3-18a) (Duro-Royo et al. [2015a]).
The extrusion shape map is defined per material and includes the extruded volume per n map repetition along a given trajectory. As a result, each extrusion length map Lt is compared to a control extrusion length Lc associated with a typical continuous extrusion. In order to determine the refill pattern of the material barrels (RP) I compute: $L_c = \sum L_t * c_s * c_t$, where cs is an estimate security coefficient (0.75) and ct is the averaged type of extrusion map that the trajectory carries. It is assigned the value of 1.00 for continuous paths and 0.25 to 0.75 for discontinuous ones. Flow rate (FR) calculations inform the pressure maps for each extrusion and a given material. Figure 3-18c illustrates the calibration of the platform with 3% concentrated chitosan polysaccharide hydrogel

material. Linear flow resulting from the relationship between flow rate and material already extruded out of the barrel can be defined by y=0.01x+1. This account is calculated for each material in the Ma and Ma' databases and used to correct the flow rate (FR) along the print job and over time (Duro-Royo et al. [2015a]).

Instructions : Once the variant and invariant parameters are calculated, local (Lo), regional (Re) and global (Gl) strategies for material heterogeneity (Figure 3-20, Figure 3-21, Figure 3-22) are implemented to structure the geometrical construct. The instruction data containing nozzle heights, time delays, and pressure maps to achieve such hierarchy is computed via Extensible Markup Language (XML) and transmitted to an instruction interface that will distribute it to both positioning (Po) and deposition (De) platforms (Figure 3-19a). The interface is designed to distribute instructions while taking into account constraints of both platforms in order to synchronize motion and extrusion for complex depositions (Duro-Royo et al. [2015a]).

The Flow of Bits : The flow of bits is initiated within a design-modeling platform and transitions to the deposition platform via serial USB communication. The deposition system (De) is located at the positioning system's (Po) end-effector and is based on a multi-barrel head digitally actuated by pneumatic hardware and circuitry. Bits flow from a micro controller (m) into relay boards (rb) that control solenoid valves (vv and vc) connected to a vacuum pump (v) and a pressure regulator (r) that receives a constant supply of airflow from an air compressor (c). Each vc valve outputs pressure to a given material barrel. Pressure levels enable start and stop deposition with positive and negative pressure respectively (Figure 3-19a). The pressure regulator (r) transforms the flow of bits into flow of pressure and receives variable impulses that determine different regional extrusion geometries with tunable heights and widths along the trajectory (Figure 3-21a).The regulator's pressure response (P) is empirically regulated when given input values from 0 to 4000 of type 16-bit unsigned integer, that correspond to 4 to 20mA of electrical current (I). A linear interpolation is then performed as follows; $I = I_0 + (I_1 - I_0) * (P - P_0/P_1 - P_0)$, so that the flow of pressure is mapped onto the flow of bits (Duro-Royo et al. [2015a]).

The Flow of Motion : Motion flow is transmitted from the instruction interface via an Ethernet UDP socket to the positioning platform every 0.012s. The positioning platform is instructed to follow complex paths made of points, lines, poly-lines or curves through different motion instructions, starting from a point in space called home (H). The motion types can be M0 (composed of multiple targets), M1 (composed of a single target), S0 (a static motion), and R0 (a reservoir refill motion) (Figure 3-19). The M0 motion spans the first trajectory target (T1), and carries the total length of the trajectory ensuring smooth positioning even if the trajectory is composed of multiple targets (Tn). A static motion S0 carries the amount of instruction cycles in order for the system to remain static. This avoids repetition of identical instructions to be sent, and therefore makes the allocation less computationally intensive, as the internal instruction file is substantially reduced in size. A refill motion R0 targets the same custom point in space and awaits for user action indicating that the reservoir, or reservoirs, are refilled properly and further action can take place (Figure 3-19) (Duro-Royo et al. [2015a]).

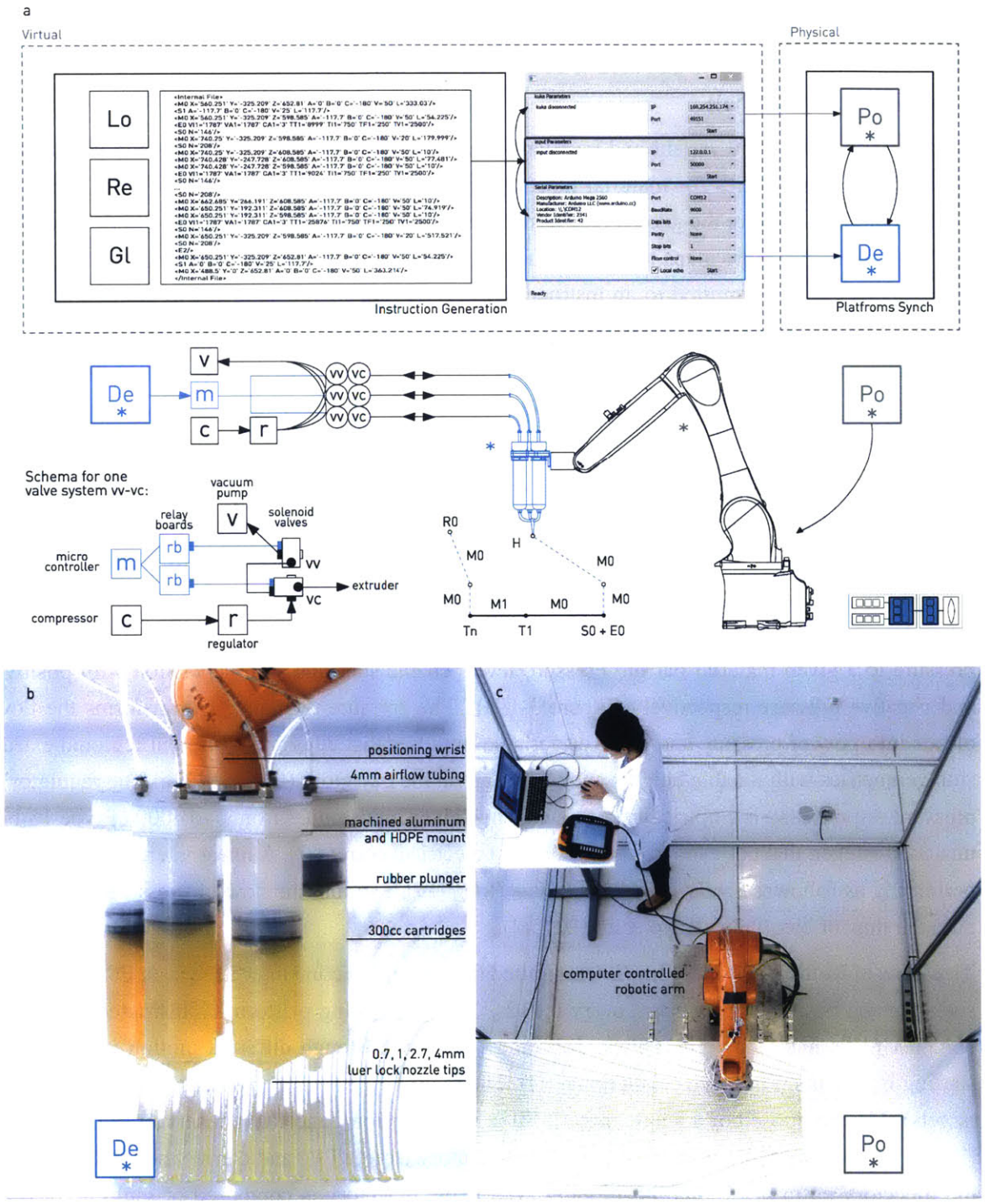

Figure 3-19: (a) The virtual model operates at three levels of resolution; local (Lo), regional (Re) and global (Gl) to fabricate heterogeneous structured objects. These hierarchical computation results are converted to fabrication instructions that are fed to a distribution interface that coordinates both positioning (Po) and deposition (De) platforms. The physical construct is achieved by implementing pressure (v,c,r), electrical (m), extrusion (E0) and motion (M0, M1, S0, R0, T1, Tn) data flows that tightly link both platforms. (b) In an exemplar application of the presented framework, a 6-barrel multi-material deposition system (De) is custom designed, built and attached to a robotic arm. (c) The computer-controlled robotic arm acts as the positioning system (Po) and receives instructions from the distribution interface in synchrony with the deposition system (De). Figure from Duro-Royo et al. [2015a].

The Flow of Pressure : Each extrusion path is designed such that it can define different extrusion shapes and material properties from base materials (Ma) or from new combinations of base materials (Ma'). This is due to the fact basic curve primitives (Figure 3-21b) are assigned material properties in the model as opposed to processes, which take as input polygonal meshes. The flow of motion and pressure can vary while following the primitives providing different speeds, extrusion forces, and material volumes from each reservoir. From a positive pressure source (air compressor, c) and a negative pressure source (vacuum pump, v) airflow is transmitted into the system's valves in order to deposit materials in different levels of organization (Figure 3-19a). At the local level, different materials in different concentrations, and diverse layering strategies can be assigned to distribute material along trajectories (Duro-Royo et al. [2015a]).
Figure 3-20a demonstrates different layering deposition strategies providing structural hierarchy within the construct. A gradient of local stiffness given by material concentration (1% to 12% in aqueous solution) is depicted in Figure 3-20b and its instances identified in a dried construct. Regional levels of control are achieved by differentiating extrusion geometries in height and width through pressure and motion flow maps. The regional pressure flow is described by three main classes (Figure 3-21d): a data allocator is in charge of reading the motion and deposition instructions (At) at the beginning of each complex path, taking around 5ms. Then a regulator sets the initial pressure (Rt) pausing the program with a 1s delay, and any other required pressures are set (Tt) to fulfill multiple variant flow maps over a trajectory (Figure 3-21d, Figure 3-21e). Airflow control is achieved through a set of valves that set initial extrusion inertia (It), remain open through the extrusion time, finalize the extrusion accounting for material inertia (Ft), and perform negative pressure to stop the material flow (Vt) (Figure 3-21d). As a result, the air flow controller time is the defined by A = C + V, where C = It + Tt - Ft, and V = Vt. It is important to note that the capabilities of pressure allocator, regulator, and controller are processed in quasi-parallel computation through sleep timers over a given trajectory (Figure 3-21d) (Duro-Royo et al. [2015a]).

The Flow of Time : The flow of time is tied to the flow of pressure. Graphs describing pressure distribution (PSI) and height distribution (Z) over time inform the height and width of regional extrusion geometries (Figure 3-21c). The minimum and maximum bound of the pressure axis is determined by the empirical material calibration data with each of the system's nozzles. The graphs describe changes in the time it takes to complete each path trajectory. They are encoded in mathematical formulas where pressure P is dependent on time T; continuous ($P = a$), incremental ($P = a * T + b$), exponential ($P = Ta$), sinusoidal ($P = a * sin(b * T + c)$), etc. that the customized firmware, loaded in the pneumatics micro controller, is able to interpret. The encoding is achieved through geometric 2D to 3D mapping. In this the case, time and flow mapping instructions transform simple curve primitives (Figure 3-21a) into 3D extrusion shapes with variable height and width along deposition trajectories (Figure 3-21e) (Duro-Royo et al. [2015a]).

The Flow of Water : Materials are evaluated with viscosities ranging from 500cPs to 50.000cPs at room temperature such as hydrogels, gel-based composites, certain types of clays, organic pastes, resins, polyvinyl alcohols etc. These materials are water-based and undergo slow curing from pastes

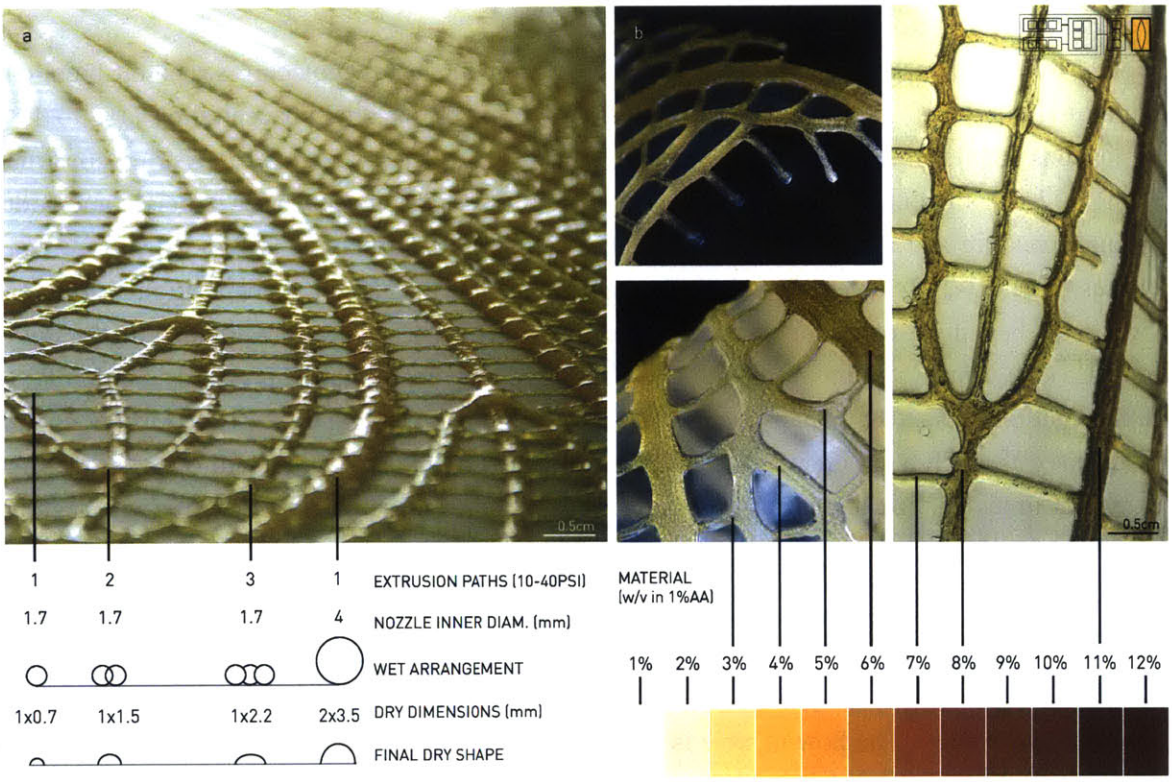

Figure 3-20: (a) An example deposition is analyzed to demonstrate material distribution patterns in cross section and resulting dry constructs. The material used in this example is an hydrogel, consequently, the volume of the deposition is significantly reduced after curing. (b) Different concentrations of polysaccharide hydrogel in mild acidic solutions can be employed to generate a gradient of materials with different opacities, viscosities and stiffness. Figure from Duro-Royo et al. [2015a].

to solids at room temperature (Mogas-Soldevila et al. [2014]). Global levels of control are achieved by the effect of combined local and regional strategies. Global shapes are reveled in the constructs when the contents of water and solvents of the materials evaporate into the environment. Single material dried extrusions of the same contour shapes with different internal patterns achieve different global shapes due to varied material distributions (Figure 3-22a). Multi-material geometries where different wet concentrations are placed side-by-side in a longitudinal manner, achieve significant curvature changes after drying (Figure 3-22b). Multi-material constructs where structural members are assigned high strength materials and infill surfaces are assigned low strength materials achieve controlled degrees of curvature after drying (Figure 3-22c). In highly complex large-scale networks, overall curvature is informed by the boundary conditions and the geometrical patterning of internal structures, in addition to multi-material deposition informed by desired structural requirements (Figure 3-22d) (Duro-Royo et al. [2015a]).

3.5.4 HFP Discussion

The integrated file-to-fabrication workflow presented here is initiated at the designer's CAD software environment and finalized at the DDM technology's operations control. It negotiates shape and material attributes with the DDM technology's mechanical constraints within a single representation and computational environment. The workflow is bidirectional in the sense that is can be implemented for top-down or bottom-up control. Specifically it can process constraints as inputs to generate performance-based fabrication outputs and at the same time it can process performance-based fabrication inputs to generate constraint outputs. When combined, this bidirectional workflow can enable powerful material and site-specific products (Duro-Royo et al. [2015a]).
In addition, the workflow is designed to control the deposition of both continuous and discontinuous printing modes to support functional gradation. This is achieved through the deposition of materials with variable mechanical properties, through the deposition of single or multiple layers and, finally, through extrusion geometry specifications given by the nozzle shape at the tip.
When generalized, the workflow can support DDM of a wide range of materials, deposition platforms and nozzle designs spanning various application domains characterized by optimal synchronization between the CNC platform and the extrusion system (Duro-Royo et al. [2014a]). The multi-material extrusion system (De) can be rapidly mounted on multiple 3-axis CNC platforms (Po) and take advantage of their precise positioning hardware. The attachment to the platform's end-effector can be customized and only requires mechanical means (Figure 3-22b, Figure 3-19c). The application of multiple materials and composites provides promising initial validation of the enabling technology and its virtual-to-physical workflow (Duro-Royo et al. [2015a]).
Design principles and methods underlying the general model and workflow are defined at the intersection of multiple research areas such as Digital Design, Computer Science, Mechanical Engineering and Materials Science and Engineering. This rich plexus of knowledge contributes to the generation of complex CAD tools, techniques and technologies tailored to provide large-scale high-definition (LSHD) for complex 3D designs (Duro-Royo et al. [2015a]).

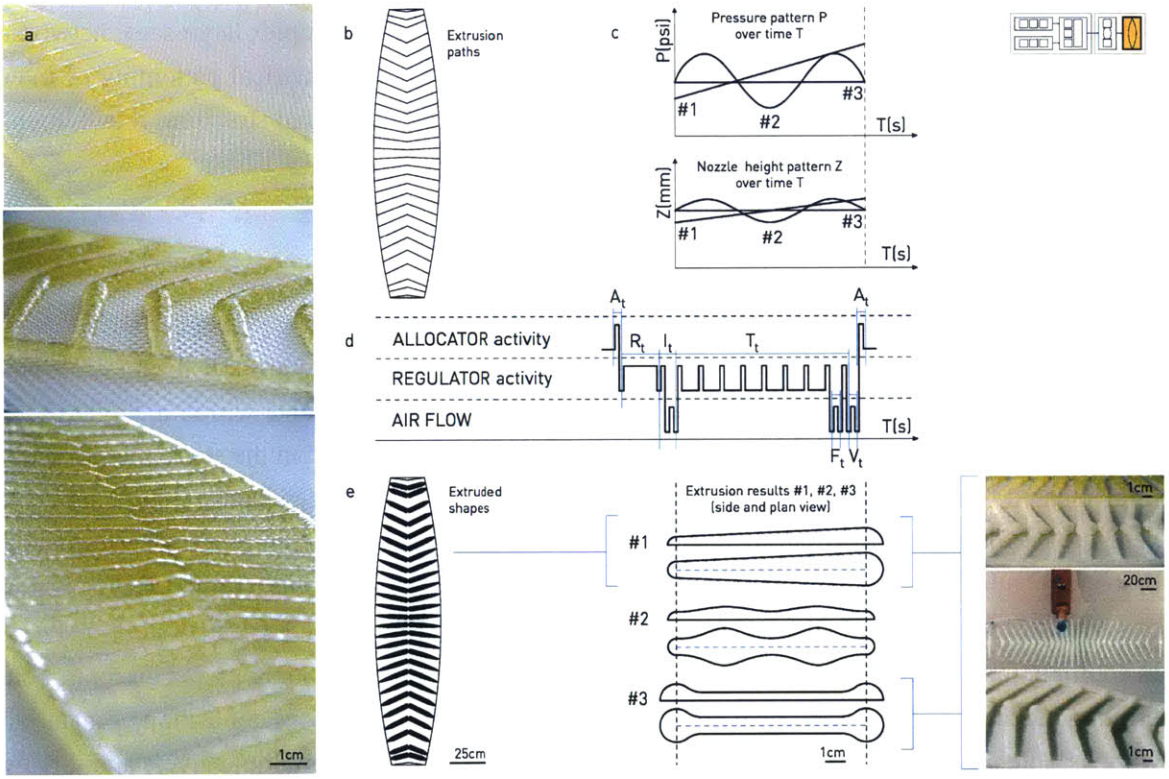

Figure 3-21: a) Regional-based control is achieved by differentiating extrusion geometries in height and width through variable pressure and motion maps. The examples shown use an hydrogel based material right after being extruded (polysaccharide hydrogel in 9% w/v in 1% acidic solution). (b) Geometrical designs are composed of simple geometries such as points, curves and lines and interpreted by the model into variable extrusion constructs. (c) The extrusions can be incremental (#1), sinusoidal (#2) or follow any other pressure map P(psi) such as #3. They can also follow nozzle height maps Z(mm) in order to result in variable material distribution extrusions. (d) In order to achieve such diversity time-dependent actions are performed in parallel. (e) The resulting extrusion shapes produce a variety of 3D configurations from simple line trajectories. Figure from Duro-Royo et al. [2015a].

3.5.5 HFP Model Results

The integrated system and workflow can achieve a continuous and seamless multi-dimensional design-to-fabrication data flow (Figure 3-17). Based on system invariant constraints and decision-driven variant input sets (Figure 3-18), a hierarchical model is implemented operating at three levels of resolution defined as local, regional and global. Basic geometric primitives are associated with diverse materials and extrusion shapes where; local refers to the way material is deposited in gradients and layering patterns (Figure 3-20), regional refers to the 3D shapes in which material can be extruded (Figure 3-21), and global refers to the topologic effects of material organization, combining both local and regional strategies (Figure 3-22). Based on these domain definitions inter-related meta-data is encoded into transmission instructions that synchronize motion and deposition platforms (Figure 3-19) to produce heterogeneous structured objects with viscous water-based materials. It is important to note that 3D constructs and complex material organization will emerge, not by direct 3D modeling, but by meta-data informing the manufacturing process with its different motions, variable pressures and diverse material compositions to deposit (Figure 3-21, Figure 3-22) (Duro-Royo et al. [2015a]).

Local : By fine-tuning mechanical property gradients and layered compositions of multi-material extrusions local hierarchical control is achieved. Figure 3-20a illustrates hierarchical deposition. Material distribution patterns and resulting dry constructs are shown in cross section and. In Figure 3-20b different concentrations of polysaccharide hydrogel in mild acidic solutions are employed to generate a gradient of materials with varying degrees of stiffness, viscosity and opacity. Unique mechanical behaviors emerge along the structures by associating and assigning these materials to the designed geometries (Duro-Royo et al. [2015a]).

Regional : Regional-based control is achieved by differentiating extrusion geometries in height and width through variable pressure and motion. The examples illustrated in Figure 3-21a are of hydrogel based material immediately following its extrusion. Figure 3-21b demonstrates designs composed of simple geometries such as points; curves and lines interpreted by the model into variable extrusion constructs, as shown in Figure 3-21a. The extrusions can be incremental (#1), sinusoidal (#2) or follow other pressure maps P(psi) such as given in #3. They can also follow nozzle height maps Z(mm) in order to achieve variable material distribution (Figure 3-21c). Variations in mechanical and optical properties are enabled by time-dependent actions performed in parallel. A data allocator reads the instructions first, based on allocation time (At). A regulator then sets initial pressure units (Rt) and any other required pressures (Tt) implementing the desired flow maps over a given trajectory. Airflow control is achieved through a set of valves that require time to set initial extrusion (It), stay open through the extrusion time, finalize the extrusion accounting for material inertia (Ft), and apply negative pressure to stop the material flow (Vt) (Figure 3-21d). The resulting extrusion shapes produce a variety of 3D configurations from simple line trajectories. In the example, the lines from Figure 3-21b are deposited in type #1 extrusions using a hydrogel-cellulose composite (Figure 3-21e) (Duro-Royo et al. [2015a]).

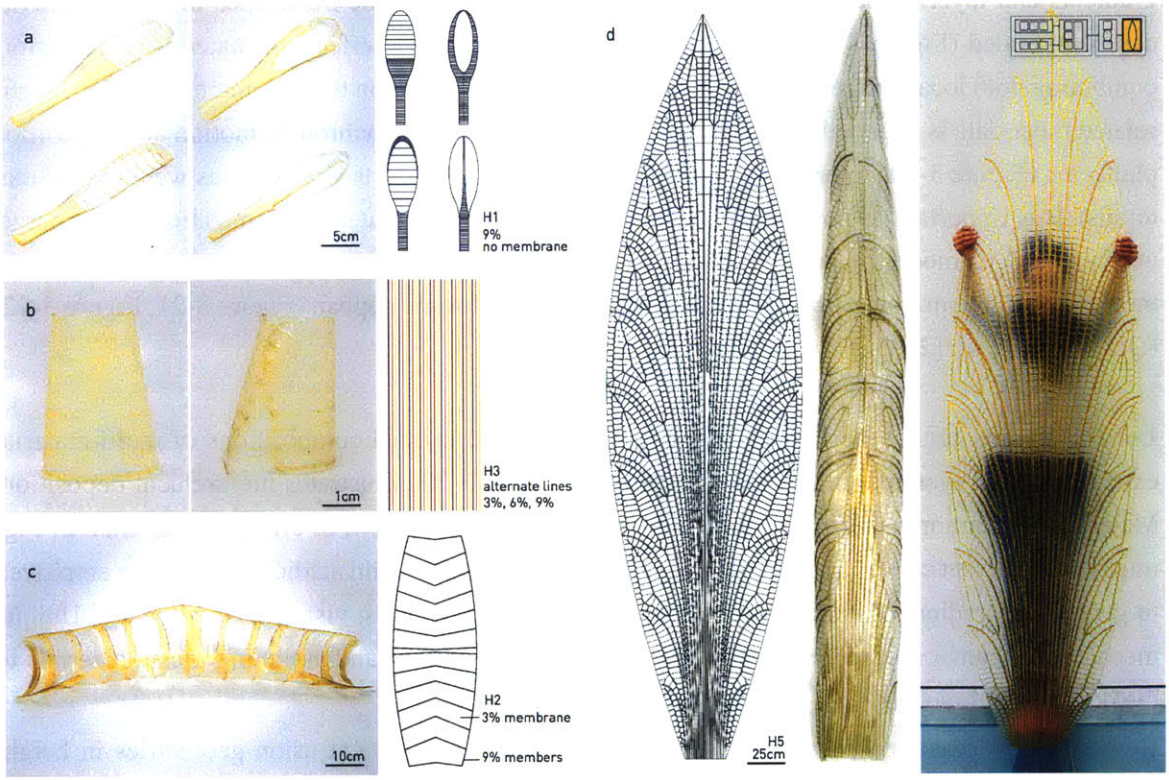

Figure 3-22: (a) Single material dried extrusions of identical global shapes defined by their boundaries, but with different internal patterns, achieve different global shapes due to varied material distributions. The material used for these examples is a polysaccharide hydrogel. (b) Multi-stiffness polysaccharide hydrogel geometries combining various concentrations (3%, 6% and 9% w/v in mild acidic solution) demonstrate form finding of tubular global shape by means of longitudinal geometric patterning and material shrinkage by water evaporation. (c) A multi-material construct in two levels of hierarchy combines high strength materials at the structural members (9% hydrogel) and low strength materials as infill skin (3% hydrogel) is deposited flat following line trajectories, and form-found due to the shrinkage of the material distributions and its geometric design. (d) A complex large-scale self-supporting construct designed as a cantilevering structure has its curvature defined by geometrical patterning and multi-material deposition in five levels of hierarchy informed by structural stability requirements. Figure from Duro-Royo et al. [2015a].

Figure 3-23: 2D tool path designs and their 3D fabricated counterparts using the HFP model.

Global : Global-based control is achieved by combining local and regional deposition strategies within global shapes. Figure 3-22 shows heterogeneously structured multi-functional objects. Different materials with different structural capacities are deposited at different levels of hierarchy ranging from one to five. The material distribution geometries and material properties defined for each deposition trajectory inform the final global shape. For instance, in Figure 3-22a, the same global shape is structured with different internal patterns and the cured constructs display corresponding global shapes induced by the shrinking forces of each pattern. In Figure 3-22b, water-based gels with different concentrations are deposited in a plane, to produce a dried tubular shape. In Figure 3-22c, tubular structural elements and surface elements are designed with two materials deposited in a spinal pattern; a stiff rubber-like gel and a light film-forming gel. Incremental pressure maps are used to deposit higher amounts of material in the center of the spine trajectories, which induced a controlled deformation pattern providing structural inertia to the construct. In Figure 3-22d, a large-scale structure is extruded with five levels of hierarchy as shown in Figure 3-20a. Its structural pattern is inspired by insect wing or leaf venation structures, and its final global shape demonstrates controlled folding into a robust and lightweight cantilever beam configuration (Duro-Royo et al. [2015a]).

HFP introduces a novel workflow for direct additive manufacturing of multifunctional heterogeneously structured objects. The workflow enables the design and digital fabrication of structural parts made of water-based materials characterized by spatial and material complexity (Figure 3-23), and at its core the workflow integrates virtual data with physical data enabling real time calibration

of data and material flow, importantly pointing towards a new design methodology characteristic of Fabrication Information Modeling (FIM) (Duro-Royo et al. [2015a]).
Through the implementation of this workflow I demonstrate the design and direct additive manufacturing of structurally patterned lightweight shells spanning overall distances of 10-feet, with a minimum amount of support, and thin cross-sections (Figure 3-22) (Duro-Royo et al. [2015a]).

Chapter 4

Towards a FIM Methodology

4.1 Analysis of Exemplar Cases of FIM

Designs based on the FIM approach are characterized by: (1) incorporating variables associated with design and construction media such as physical feedback sensing, fabrication and material parameters; (2) operating across multiple dimensions; and, (3) integrating and managing trans-disciplinary data parameters, constraints, or data sets from multiple disciplines. Below I analyze and integrate key strategies employed in each of the models. I relate to the three main principles of FIM: (1) multidimensionality, (2) trans disciplinary data integration and, (3) material-informed computation.

4.2 Multi-dimensional Characteristics

In the FCA model, a scaffold is created with local differenced thread distributions using robotic weaving techniques. The weaving patterns and distances between threads are informed by typical physiological spinning ranges observed in live silkworms. Six thousand five hundred ready-to-spin silkworms are deployed onto the scaffold and produce a silken dome with throughout density variations steered by local changes in woven structure (Figure 4-1 top). A similar local-to-global strategy is implemented in the STP model. In this case, unit-level geometric features are dependent on, and negotiated within, higher-level assemblies; so that interlocks and overlaps are preserved keeping the whole construct functional and flexible (Figure 4-2 top). In the SPS model, a virtual a-dimensional rule-based behavioral system generates local rules for global coordination of agents. This results in agents achieving construction of a whole structure without top-down control (Figure 4-3 top). The HFP model is the one that spans most dimensions in disciplines and scales. The chemical makeup of polymers is designed and modulated at the nano-scale, use their material properties to allow for full bonding across printed sections, and then control global structural emergence of shape via hydration patterns at the architectural scale (Figure 4-4 top) (Duro-Royo et al. [2015b]).

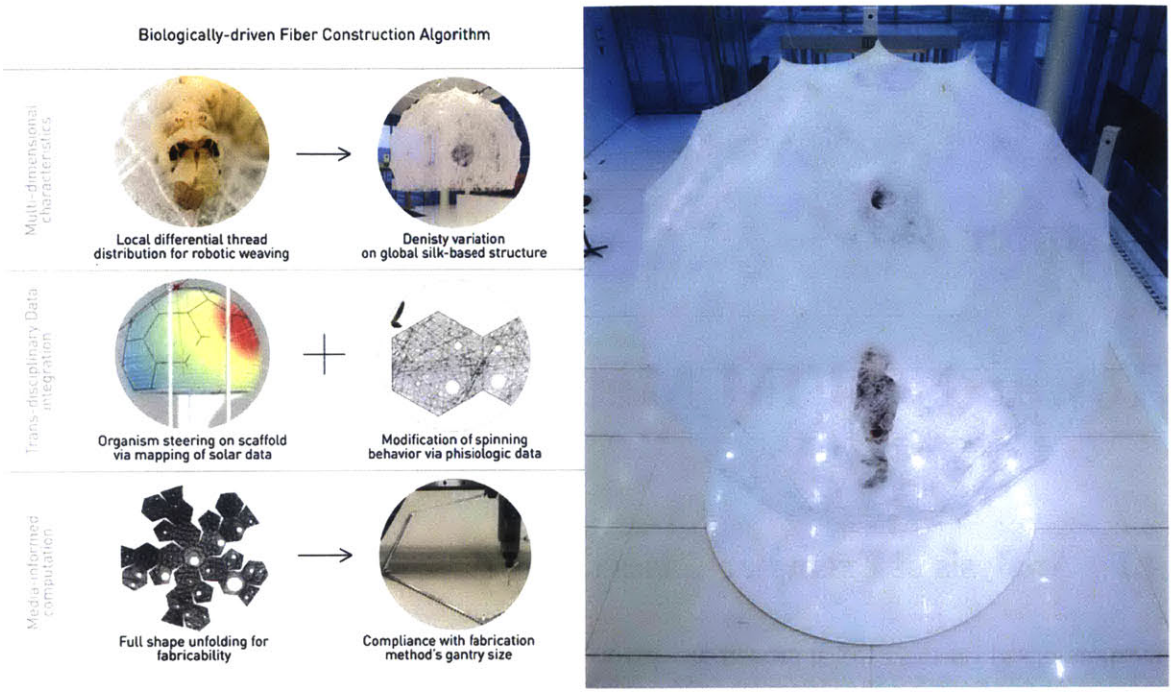

Figure 4-1: Biologically-driven Fiber Construction Algorithm (FCA) analyzed in terms of multi-dimensionality, trans-disciplinary data integration and media-informed computation. Figure from Duro-Royo et al. [2015b].

4.3 Trans-disciplinary Data Integration

Efficient and timely integration of trans-disciplinary information is fundamental to the development of workflows that integrate media-informed designs across complex dimensions. In the FCA model, two main data sets are integrated into the design applet. The first one considers solar radiation for a given period of time relative to the surface of a dome scaffold, and the second one encodes the typical physiological ranges of silkworm spinning as explained above. The combination of both environmental and biological data sets allows the design to seamlessly combine environmental and biological considerations (Figure 4-1 middle). In the case of the STP model, morphometric data from a material science driven study of the scales of a prehistoric fish is parameterized and categorized to respond to geometrical features. Principal and secondary directions for the emergence of interlock and overlap features are then linked to functional requirements in new synthetic designs (Figure 4-2 middle). Both in SPS and HFP, structural design data is integrated in the models. In SPS, rules for structural design intent are introduced as typological "steering forces" affecting the swarm-based printing system (Figure 4-3 middle). In HFP, the principal load distributions of simple structural typologies, such as cantilevers or post-and-beams, are combined and encoded into streamline gradients that produce structural support gradients in the final manufactured objects (Figure 4-4 middle) (Duro-Royo et al. [2015b]).

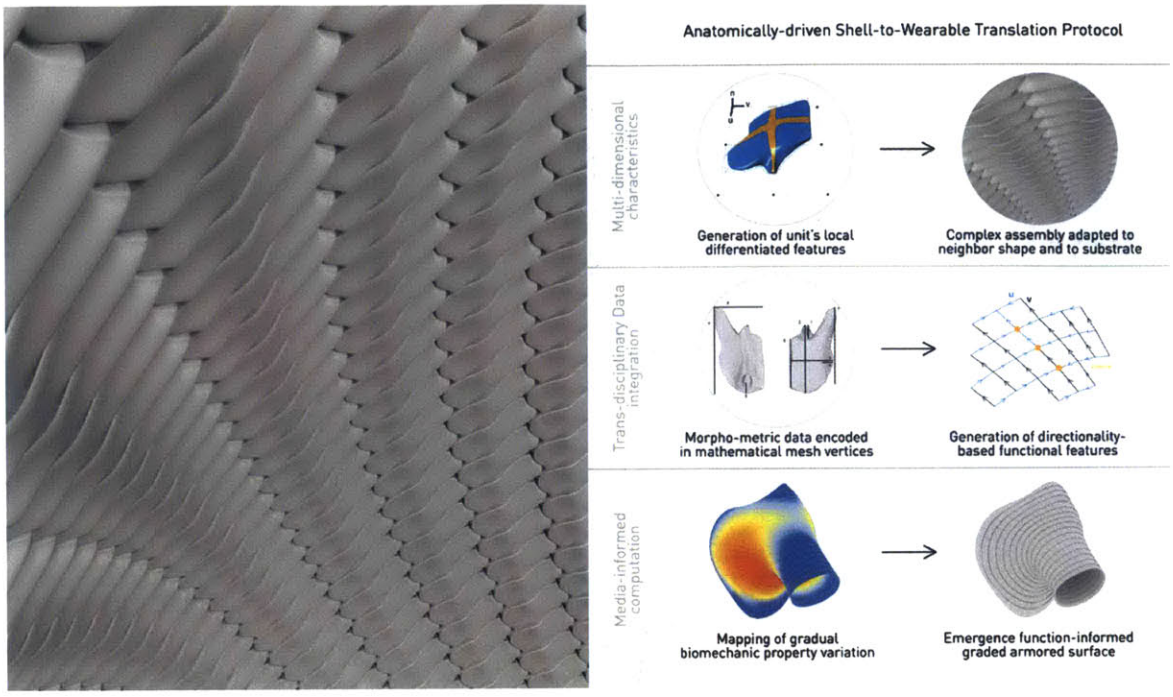

Figure 4-2: Anatomically-driven Shell-to-Wearable Translation Protocol (STP) analyzed in terms of multi-dimensionality, trans-disciplinary data integration and media-informed computation. Figure from Duro-Royo et al. [2015b].

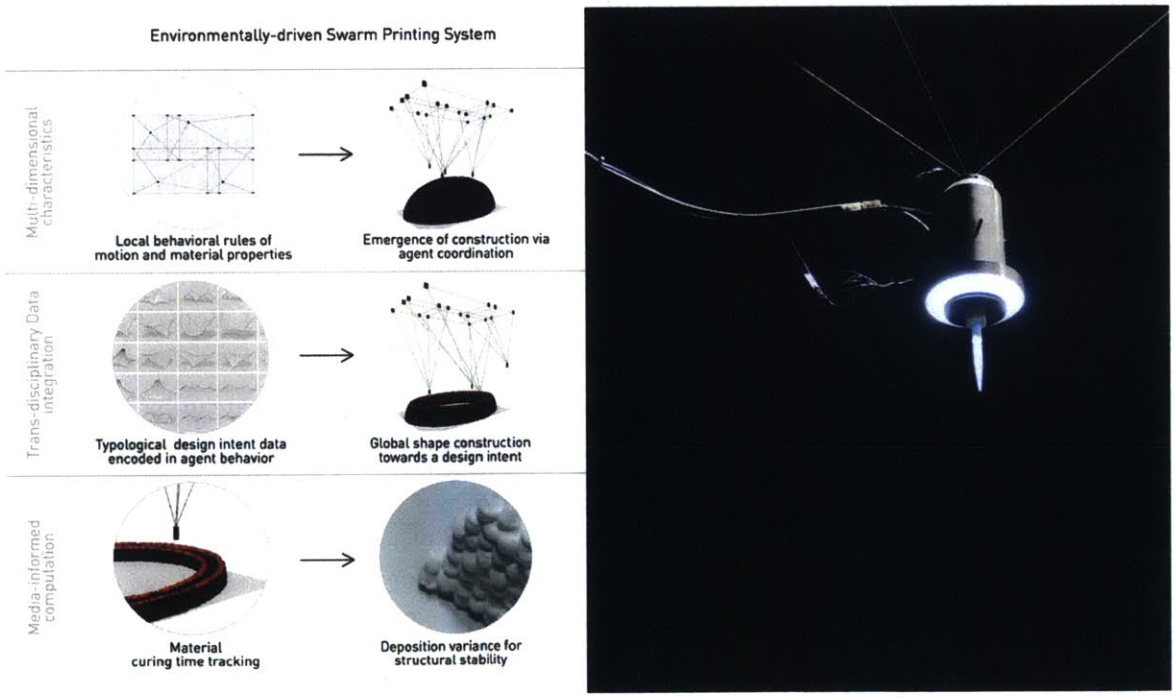

Figure 4-3: Environmentally-driven Swarm Printing System (SPS) analyzed in terms of multi-dimensionality, trans-disciplinary data integration and media-informed computation. Figure from Duro-Royo et al. [2015b].

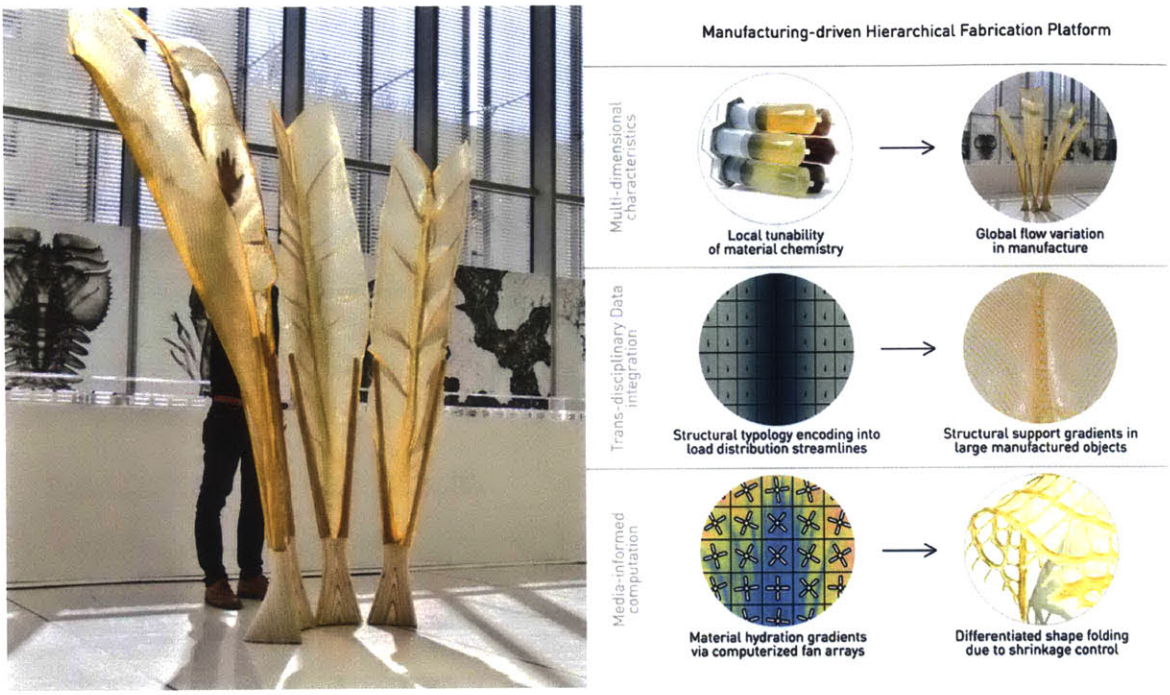

Figure 4-4: Manufacturing-driven Hierarchical Fabrication Platform (HFP) analyzed in terms of multi-dimensionality, trans-disciplinary data integration and media-informed computation. Figure from Duro-Royo et al. [2015b]

4.4 Media-informed Computation

In order to design and materialize complex projects such as natural silk domes, biopolymer cantilevers, or articulated armors, design models must incorporate material-, and fabrication-informed parameters into computational models. In the FCA model I implement a functionality that unfolds the structure and coordinates the robotic weaving of 26 frames composing a full-scale dome. The algorithm is made fully "aware" of machine gantry dimensions, speeds, and feeds (Figure 4-1 bottom). In the STP case, functional maps inform computation of geometric negotiations within the scale-based system. The maps can encode bio-mechanic requirements of breathability, opacity, or flexibility and protection, on the surface of a human chest (Figure 4-2 bottom). Both SPS and HFP incorporate novel material-informed computation strategies. In SPS virtual clocks track material extrusion of drops in position and runtime in order to calculate estimated final curing times. The agents in the system are computed to obtain this data avoiding the deposition of new material drops on top of the uncured ones so that structural stability is guaranteed (Figure 4-3 bottom). In HFP, the levels of hydration of the de-posited polymers are controlled by convection systems that target different areas of the structure. Such differential convection allows for shrinkage control of the polymers as they dry, so that final shaping can be induced in certain areas (Figure 4-4 bottom) (Duro-Royo et al. [2015b]).

Chapter 5

Reflections on Fabrication Information Modeling (FIM)

I envision Fabrication Information Modeling (FIM) as a novel framework and methodology for materially and geometrically complex design, as a way to combine form generation, digital fabrication, and material computation in seamless digital design processes. The challenges associated with the projects described and analyzed in this thesis can be grouped into types of limitations associated with virtual design environments. The first set of limitations arises when attempting to integrate design variables from a wide array of disciplines such as material science, mechanical engineering, biology or structural design (e.g. in FCA, SPS, STP and HFP models); the second set of limitations arises from challenges associated with adapting shape-based parameters to digital fabrication and computer aided machining constraints (e.g. in FCA, SPS and HFP models); the third set of limitations arises when aiming to intervene at different scales of time, resolution and representation (e.g. in SPS and STP models).

The challenges in achieving design synthesis across media, scales and disciplines are many, and typically, they are the result of following computer-aided design traditions that should be adapted to, or replaced by, novel ways to understand and implement physical feedback workflows. **With FIM, I aim to design and build physical feedback workflows where materials are designed rather than selected; where the question of how information is passed across spatiotemporal scales is central to the design generation process itself; where modeling at each level of resolution and representation is based on various (and often complimenting) methods, and performed by different agents within a single environment; and finally, where virtual and physical considerations coexist as equals.**

5.1 Future Work Towards FIM

Initial results from the analysis of four case studies of FIM demonstrate functional integration, multi scale performance and novel aesthetic qualities. I anticipate that additional research in this area will

point towards advancing the capabilities of computational design and digital fabrication workflows with real-time multi-scale trans-disciplinary data.

5.1.1 FCA Model Future Work

Further research into biologically driven fiber construction algorithms (FCA) will explore various techniques for using templates in biological fabrication in order to generate highly controlled and tunable functional gradients of material properties. New types of high-performance textile composites may be designed in this way, not unlike the composites observed on the pavilion which combine internal and external natural-silk wrapping of the synthetic threads. Finally, with regard to decentralized swarm-like construction processes similar to the ones viewed in nature, future developments in the potential of collaborative construction behavior will be further explored.

5.1.2 STP Model Future Work

The anatomically driven shell-to-wearable translation protocol (STP) is constructed on the logic of a biological system rather than provide for a specific bio-inspired design solution. The model can be used to incorporate real physiological data and kinetic schema from the human body. In future implementations the hierarchical structure of STP enables incorporation of other concepts relevant to human physiology, such as the Lines of Non-Extension (LNE) (Iberall [1970]). In ongoing research on the STP model I am building continuity between computational construction and additive fabrication. The model preserves the closed mesh articulation and the relation amongst the units, but does not yet accommodate material articulation strategies such as layered microstructures, graded material interfaces, and internal porosity. Yet, STP's hierarchical organization provides the platform for additional meta organization principles at the local, regional, and global levels of the design process.

5.1.3 SPS Model Future Work

In future implementations of the environmentally driven swarm printing system (SPS), sensing feedback can play a key role in the design and development of the agents' rule-based behavior. By means of 3D scanning and thermal imaging, structural stability and material behavior can be monitored and fed back into the model. Real-time comparison of virtual and physical built volumes, as well as the aforementioned material property tracking function, can contribute to closing the gap between virtual-to-physical design workflows; as well as opening up new and exciting opportunities for innovative long-distance fabrication environments where the designer provides input from afar.

5.1.4 HFP Model Future Work

For future applications of the manufacturing-driven hierarchical fabrication platform model (HFP) we plan to explore additive manufacturing of solid structures constructed out of a wider range of structural materials. In terms of local structural controls future research will focus on enhancing

material complexity at micro- and nano-scales combining micro layering of specific material structures and properties to produce high resolution composites inspired by natural structures such as nacre or silk (Pottmann et al. [2008]). In particular I am excited about the possibility of reversing the design workflow to enable formal iterations to the virtual model. This feature will aid closing the loop characteristic of the file-to-factory paradigm and will promote a factory-to-file methodology thereby further refining the workflow as feedback-enabled. Such feedback positive workflow will incorporate interrogative methods such as environment-specific and performance-based predictive modeling (Bethke et al. [2005]). Furthermore, the effect of temperature, humidity, light or airflow can be modeled at the global level of resolution thereby informing both local and regional features. Global shape outcomes could then be visualized in the virtual model for informed design decision-making prior to final fabrication. Such closed loop fabrication workflows will contribute not only to a substantial improvement of virtual-to-physical flow field computation, but will also offer insight into the way in which CAD platforms for HOM are designed and implemented.

Biography

Jorge Duro Royo is a Research Assistant at the Mediated Matter group, MIT Media Lab, where he focuses on novel virtual-to-physical theoretical and applied digital design methods under the umbrella of Fabrication Information Modeling (FIM). He studied Architecture as the Polytechnic University of Catalonia, School of Architecture (UPC-ESTAV) and Mechanical Engineering at the Polytechnic University of Catalonia, School of Industrial and Aeronautic Engineering (UPC-ETSEIAT) where he graduated with honors with a focus on structural design and construction. Since 2010 he has taught introductory hands-on courses on Digital Visualization, Parametric Architecture, and Computational Design, and collaborated with diverse academic research groups at the Massachusetts Institute of Technology, Harvard University and Tufts University.

Bibliography

Hazem M N Afify, Zeinab A A B D Elghaffar, and C A D Cam. Advanced digital manufacturing techniques (cam) in architecture authors hazem m. n. afify and zeinab a. abd elghaffar. In *Embodying Virtual Architecture: ASCAAD 's Third International Conference on Computing in Architectural Design*, 2007.

Alfredo Andia and Thomas Spiegelhalter. *Post-parametric automation in design and construction.* Boston ; London : Artech House, [2015], 2015. ISBN 1608076938.

Federico Augugliaro, Sergei Lupashin, Michael Hamer, Cason Male, Markus Hehn, Mark W Mueller, Jan Sebastian Willmann, Fabio Gramazio, Mark Kohler, and Raffaello D'Andrea. The flight assembled architecture installation: Cooperative construction with flying machines. *Control Systems, IEEE*, 34(4):46–64, 2014. ISSN 1066-033X.

Richard Beckett and Sarat Babu. To the micron: A new architecture through high-resolution multi-scalar design and manufacturing. *Architectural Design*, 84(1):112–115, 2014. ISSN 00038504.

Kristen Bethke, Dava J Newman, and Raul Radovitzky. Creating a skin strain field map with application to advanced locomotion spacesuit design. In *Proceedings of the XXth congress of the international society of biomechanics (ISB), Cleveland, OH*, 2005.

Arpan Biswas, Vadim Shapiro, and Igor Tsukanov. Heterogeneous material modeling with distance fields. *Computer Aided Geometric Design*, 21(3):215–242, 2004. ISSN 01678396.

Jack E Bresenham. Algorithm for computer control of a digital plotter. *IBM Systems journal*, 4(1): 25–30, 1965. ISSN 0018-8670.

Mark Burry, Sambit Datta, and Simon Anson. Introductory Computer Programming as a Means for Extending Spatial and Temporal Understanding. In *Eternity, Infinity and Virtuality in Architecture Proceedings of the 22nd Annual Conference of the Association for Computer-Aided Design in Architecture (ACADIA)*, pages 129–135, Washington D.C, USA, 2002.

C C Chang. Direct slicing and G-code contour for rapid prototyping machine of UV resin spray using PowerSOLUTION macro commands. *The International Journal of Advanced Manufacturing Technology*, 23(5-6):358–365, 2004. ISSN 0268-3768.

W. K. Chiu and K. M. Yu. Direct digital manufacturing of three-dimensional functionally graded material objects. *Computer-Aided Design Journal*, 40(12):1080–1093, 2008. ISSN 00104485.

Steven W Cranford and Markus J Buehler. *Biomateriomics. [electronic resource].* Springer series in materials science: 165. Dordrecht : Springer, c2012., 2012. ISBN 9781283740982. URL `http://goo.gl/vHvY4C`.

Jorge Duro-Royo, Laia Mogas-Soldevila, and Neri Oxman. Methods and Apparatus for Integrated Large Scale Robotic Fabrication of Functionally Graded Materials and Structures, 2014a.

Jorge Duro-Royo, Katia Zolotovsky, Laia Mogas-Soldevila, Swati Varshney, Neri Oxman, Mary C. Boyce, and Christine Ortiz. MetaMesh: A hierarchical computational model for design and fabrication of biomimetic armored surfaces. *Computer-Aided Design Journal*, 2014b.

Jorge Duro-Royo, Laia Mogas-Soldevila, Markus Kayser, and Neri Oxman. Modelling Behaviour for Additive & Distributed Digital Construction. In *Proceedings of the DMSC Design Modelling Symposium*, Copenhagen, 2015a.

Jorge Duro-Royo, Laia Mogas-Soldevila, and Neri Oxman. Flow-Based Fabrication: An Integrated Computational Workflow for Digital Design and Additive Manufacturing of Multifunctional Heterogeneously Structured Objects. *Computer-Aided Design Journal*, 2015b.

Jorge Duro-Royo, Laia Mogas-Soldevila, and Neri Oxman. Physical Feedback Workflows in Fabrication Information Modeling (FIM): Analysis and Discussion of Exemplar Cases Across Media, Disciplines and Scales. In *Real Time Proceedings of the 33rd eCAADe Conference*, volume 53, pages 1–9, 2015c.

Jacob Fish. *Practical multiscaling*. John Wiley & Sons, 2013. ISBN 1118534859.

Moritz Fleischmann, Julian Lienhard, and Achim Menges. Computational Design Synthesis: Embedding Material Behaviour in Generative Computational Processes. *Respecting Fragile Places: 29th eCAADe Conference Proceedings*, pages 759–767, 2011.

A S Iberall. The experimental design of a mobile pressure suit. *Journal of Fluids Engineering*, 92 (2):251–264, 1970. ISSN 0098-2202.

Hanif Kara and Andreas Georgoulias. *Interdisciplinary Design: New Lessons from Architecture and Engineering*. ACTAR Publishers, 2012. ISBN 8415391080.

Brian A Kidd, Lauren A Peters, Eric E Schadt, and Joel T Dudley. Unifying immunology with informatics and multiscale biology. *Nature immunology*, 15(2):118–127, 2014. ISSN 1529-2908.

Leif Kobbelt and Mario Botsch. Freeform shape representations for efficient geometry processing. In *Shape Modeling International, 2003*, pages 111–115. IEEE, 2003. ISBN 0769519091.

Quentin Lindsey, Daniel Mellinger, and Vijay Kumar. Construction of cubic structures with quadrotor teams. *Proc. Robotics: Science & Systems VII*, 2011.

Martti Mäntylä. Topological analysis of polygon meshes. *Computer-Aided Design Journal*, 15(4): 228–234, 1983. ISSN 0010-4485.

Martti Mäntylä. An introduction to solid modeling. 1988.

Robert McNeel. Grasshopper generative modeling for Rhino. *Computer software*, 2010. URL `http://goo.gl/1yNf5D`.

William J Mitchell. Vitruvlus redux: formalized design synthesis in architecture, 2001.

Laia Mogas-Soldevila. *New design companions opening up the process through self-made computation*. PhD thesis, Massachusetts Institute of Technology, 2013.

Laia Mogas-Soldevila, Jorge Duro-Royo, and Neri Oxman. Water-Based Robotic Fabrication: Large-Scale Additive Manufacturing of Functionally Graded Hydrogel Composites via Multi-chamber Extrusion. *3D Printing and Additive Manufacturing*, 1(3):141–151, 2014. ISSN 2329-7662.

Roberto Naboni and Ingrid Paoletti. *Advanced Customization in Architectural Design and Construction*. Springer, 2015. ISBN 3319044230.

Anitra Nelson, Andrew Maher, and Mark Burry. The'discipline'in interdisciplinary and transdisciplinary research. *International Journal of Interdisciplinary Social Sciences*, 1(1):147–154, 2006. ISSN 1833-1882.

Kas Oosterhuis. File to Factory and Real Time Behavior in Architecture, Fabrication: Examining the Digital Practice of Architecture. In *Proceedings of Conference of the AIA Technology in Architectural Practice Knowledge Community, Cambridge/Ontario*, pages 294–305, 2004.

Kas Oosterhuis, H H Bier, Cas Aalbers, and Sander Boer. File to Factory and Real Time Behavior in ONL-Architecture. In *Fabrication: Examining the Digital Practice of Architecture, Proceedings of the 23rd Annual Conference of the Association for Computer Aided Design in Architecture and the 2004 Conference of the AIA Technology in Architectural Practice Knowledge Community*, 2004. ISBN 0969666527.

Neri Oxman. Variable property rapid prototyping. *Virtual and Physical Prototyping*, 6(1):3–31, March 2011. ISSN 1745-2759.

Neri Oxman, Elizabeth Tsai, and Michal Firstenberg. Digital anisotropy: A variable elasticity rapid prototyping platform. *Virtual and Physical Prototyping*, 7(4):261–274, 2012. ISSN 1745-2759.

Neri Oxman, Jared Laucks, Markus Kayser, Jorge Duro-Royo, and Carlos Gonzales-Uribe. Silk Pavilion: A Case Study in Fiber-based Digital Fabrication. In *FABRICATE Conference Proceedings*, pages 248–255, 2013a.

Neri Oxman, Jared Laucks, Markus Kayser, Elizabeth Tsai, and Michal Firstenberg. Freeform 3D printing: Towards a sustainable approach to additive manufacturing. *Green Design, Materials and Manufacturing Processes*, page 479, 2013b. ISSN 1138000469.

Neri Oxman, Jorge DuroRoyo, Steven Keating, Ben Peters, and Elizabeth Tsai. Towards Robotic Swarm Printing. *Architectural Design*, 84(3):108–115, 2014. ISSN 1554-2769.

Neri Oxman, Christine Ortiz, Fabio Gramazio, and Matthias Kohler. Material ecology. *Computer-Aided Design Journal*, 60:1–2, March 2015. ISSN 0010-4485.

Helmut Pottmann, Alexander Schiftner, and Johannes Wallner. Geometry of architectural freeform structures. In *Symposium on Solid and Physical Modeling*, page 9, 2008.

Steffen Heinz Reichert. *Reverse engineering nature: design principles for flexible protection inspired by ancient fish armor of Polypteridae*. PhD thesis, 2010.

Larry Sass and Rivka Oxman. Materializing design: the implications of rapid prototyping in digital design. *Design Studies*, 27(3):325–355, 2006. ISSN 0142-694X.

Fabian Scheurer. Materializing complexity. *John Wiley & Sons*, 80:86–93, 2010.

Simon Schleicher, Julian Lienhard, Simon Poppinga, Thomas Speck, and Jan Knippers. A methodology for transferring principles of plant movements to elastic systems in architecture. *Computer-Aided Design Journal*, 60:105–117, 2015. ISSN 0010-4485.

Vadim Shapiro, Igor Tsukanov, Arpan Biswas, and Michael Freytag. Modeling and analysis of objects having heterogeneous material properties, July 2004.

Vadim Shapiro, Igor Tsukanov, and Alex Grishin. Geometric issues in computer aided design/computer aided engineering integration. *Journal of Computing and Information Science in Engineering*, 11(2):21005, 2011. ISSN 1530-9827.

R Sheil. De-Fabricating Protoarchitecture. In *Prototyping Architecture*, London, 2013. Building Centre Trust.

Pau Sola-Morales. *Representation in architecture: a data model for computer-aided architectural design.* PhD thesis, Hardvard Universtity Graduate School of Design, 2000.

Martin Tamke, Gregory Quinn, Henrik Leander Evers, Anders Holden Deleuran, and Christoph Gengnagel. The Challenge of the bespoke Design, Simulation and Optimisation of a Computationally Designed Plywood Gridshell. In *Fusion Proceedings of the 32nd eCAADe Conference*, volume 2, pages 29–38, Newcastle upon Tyne, UK, 2013.

Ying Tan and Zhong-yang Zheng. Research advance in swarm robotics. *Defence Technology*, 9(1): 18–39, 2013. ISSN 2214-9147.

Gabriel Taubin. Introduction to geometric processing through optimization. *Computer Graphics and Applications, IEEE*, 32(4):88–94, 2012. ISSN 0272-1716.

Michela Turrin, Peter von Buelow, and Rudi Stouffs. Design explorations of performance driven geometry in architectural design using parametric modeling and genetic algorithms. *Advanced Engineering Informatics*, 25(4):656–675, 2011. ISSN 1474-0346.

Justin Werfel, Kirstin Petersen, and Radhika Nagpal. Designing collective behavior in a termite-inspired robot construction team. *Science*, 343(6172):754–758, 2014. ISSN 0036-8075.

Cem Yuksel, Jonathan M Kaldor, Doug L James, and Steve Marschner. Stitch meshes for modeling knitted clothing with yarn-level detail. *ACM Transactions on Graphics (TOG)*, 31(4):37, 2012. ISSN 0730-0301.

Yongjie Zhang, Chandrajit Bajaj, and Guoliang Xu. Surface smoothing and quality improvement of quadrilateral/hexahedral meshes with geometric flow. In *Proceedings of the 14th international meshing roundtable*, pages 449–468. Springer, 2005. ISBN 3540251375.